FEEDBACK CONTROL OF A NONHOLONOMIC CAR-LIKE ROBOT*

Alessandro De Luca   Giuseppe Oriolo

Dipartimento di Informatica e Sistemistica
Università di Roma "La Sapienza"
Via Eudossiana 18, 00184 Rome, Italy
{deluca,oriolo}@labrob.ing.uniroma1.it

Claude Samson

INRIA
2004 Route de Lucioles, 06902 Sophia-Antipolis, France
Claude.Samson@sophia.inria.fr

*This material will appear as Chapter 4 of *Planning Robot Motion*, J.-P. Laumond Ed., Springer-Verlag, 1997. This book presents results from the ESPRIT Basic Research Project 6546 *PROMotion*.

Contents

1 Introduction

The subject of this chapter is the control problem for nonholonomic wheeled mobile robots moving on the plane, and in particular the use of *feedback* techniques for achieving a given motion task.

In automatic control, feedback improves system performance by allowing the successful completion of a task even in the presence of external disturbances and/or initial errors. To this end, real-time sensor measurements are used to reconstruct the robot state. Throughout this study, the latter is assumed to be available at every instant, as provided by proprioceptive (e.g., odometry) or exteroceptive (sonar, laser) sensors.

We will limit our analysis to the case of a robot workspace free of obstacles. In fact, we implicitly consider the robot controller to be embedded in a hierarchical architecture in which a higher-level planner solves the obstacle avoidance problem and provides a series of motion goals to the lower control layer. In this perspective, the controller deals with the basic issue of converting ideal plans into actual motion execution. Wherever appropriate, we shall highlight the interactions between feedback control and motion planning primitives, such as the generation of open-loop commands and the availability of a feasible smooth path joining the current robot position to the destination.

The specific robotic system considered is a vehicle whose kinematic model approximates the mobility of a car. The configuration of this robot is represented by the position and orientation of its main body in the plane, and by the angle of the steering wheels. Two velocity inputs are available for motion control. This situation covers in a realistic way many of the existing robotic vehicles. Moreover, the *car-like* robot is the simplest nonholonomic vehicle that displays the general characteristics and the difficult maneuverability of higher-dimensional systems, e.g., of a car towing trailers. As a matter of fact, the control results presented here can be directly extended to more general kinematics, namely to all mobile robots admitting a chained-form representation. In particular, our choice encompasses the case of unicycle kinematics, another ubiquitous model of wheeled mobile robot, for which simple but specific feedback control methods can also be derived.

The nonholonomic nature of the car-like robot is related to the assumption that the robot wheels roll without slipping. This implies the presence of a nonintegrable set of first-order differential constraints on the configuration variables. While these nonholonomic constraints reduce the instantaneous motions that the robot can perform, they still allow global controllability in the configuration space. This unique feature leads to some challenging problems in the synthesis of feedback controllers, which parallel the new research issues arising in nonholonomic motion planning. Indeed, the wheeled mobile robot application has triggered the search for innovative types of feedback controllers that can be used also for more general nonlinear systems.

In the rest of this introduction, we present a classification of motion control problems, discussing their intrinsic difficulty and pointing out the relationships between planning and control aspects.

1.1 Problem classification

In order to derive the most suitable feedback controllers for each case, it is convenient to classify the possible motion tasks as follows:

- *Point-to-point motion*: The robot must reach a desired goal configuration starting from a given initial configuration.
- *Path following*: The robot must reach and follow a geometric path in the cartesian space starting from a given initial configuration (on or off the path).
- *Trajectory tracking*: The robot must reach and follow a trajectory in the cartesian space (i.e., a geometric path with an associated timing law) starting from a given initial configuration (on or off the trajectory).

The three tasks are sketched in Fig. 1, with reference to a car-like robot.

Using a more control-oriented terminology, the point-to-point motion task is a *stabilization* problem for an (equilibrium) point in the robot state space. For a car-like robot, two control inputs are available for adjusting four configuration variables, namely the two cartesian coordinates characterizing the position of a reference point on the vehicle, its orientation, and the steering wheels angle. More in general, for a car-like robot towing N trailers, we have two inputs for reconfiguring $n = 4 + N$ states. The error signal used in the feedback controller is the difference between the current and the desired configuration.

In the path following task, the controller is given a geometric description of the assigned cartesian path. This information is usually available in a parameterized form expressing the desired motion in terms of a path parameter σ, which may be in particular the arc length along the path. For this task, time dependence is not relevant because one is concerned only with the geometric displacement between the robot and the path. In this context, the time evolution of the path parameter is usually free and, accordingly, the command inputs can be arbitrarily scaled with respect to time without changing the resulting robot path. It is then customary to set the robot forward velocity (one of the two inputs) to an arbitrary constant or time-varying value, leaving the second input available for control. The path following problem is thus rephrased as the stabilization to zero of a suitable scalar path error function (the distance d to the path in Fig. 1b) using only one control input. For the car-like robot, we shall see that achieving $d \equiv 0$ implies the control of three configuration variables—one less than the dimension of the configuration space—because higher-order derivatives of the controlled output d are related to these variables. Similarly, in the presence of N trailers, requiring $d \equiv 0$ involves the control of as many as $n - 1 = N + 3$ coordinates using one input.

In the trajectory tracking task, the robot must follow the desired cartesian path with a specified timing law (equivalently, it must track a moving reference robot). Although the trajectory can be split into a parameterized geometric path and a timing law for the parameter, such separation is not strictly necessary. Often, it is simpler to specify the workspace trajectory as the desired time evolution for the position of some representative point of the robot. The trajectory tracking problem consists then in the stabilization to zero of the two-dimensional cartesian error e (see Fig. 1c) using both control inputs. For the car-like robot, imposing $e \equiv 0$ over time implies the control of all four configuration variables. Similarly, in the presence of N trailers, we are actually controlling $n = N + 4$ coordinates using two inputs.

The point stabilization problem can be formulated in a local or in a global sense, the latter meaning that we allow for initial configurations that are arbitrarily far from the destination. The same is true also for path following and trajectory tracking, although locality has two different meanings in these tasks. For path following, a local solution means that the controller works properly provided we start sufficiently close to the path; for trajectory tracking, closeness should be evaluated with respect to the current position of the reference robot.

The amount of information that should be provided by a high-level motion planner varies for each control task. In point-to-point motion, information is reduced to a minimum (i.e., the goal configuration only) when a globally stabilizing feedback control solution is available. However, if the initial error is large, such a control may produce erratic behavior and/or large control effort which are unacceptable in practice. On the other hand, a local feedback solution requires the definition of intermediate subgoals at the task planning level in order to get closer to the final desired configuration.

For the other two motion tasks, the planner should provide a path which is kinematically feasible (namely, which complies with the nonholonomic constraints of the specific vehicle), so as to allow its perfect execution in nominal conditions. While for an omnidirectional robot any path is feasible, some degree of geometric smoothness is in general required for nonholonomic robots. Nevertheless, the intrinsic feedback structure of the driving commands enables to recover transient errors due to isolated path discontinuities. Note also that the unfeasibility arising from a lack of continuity in some higher-order derivative of the path may be overcome by

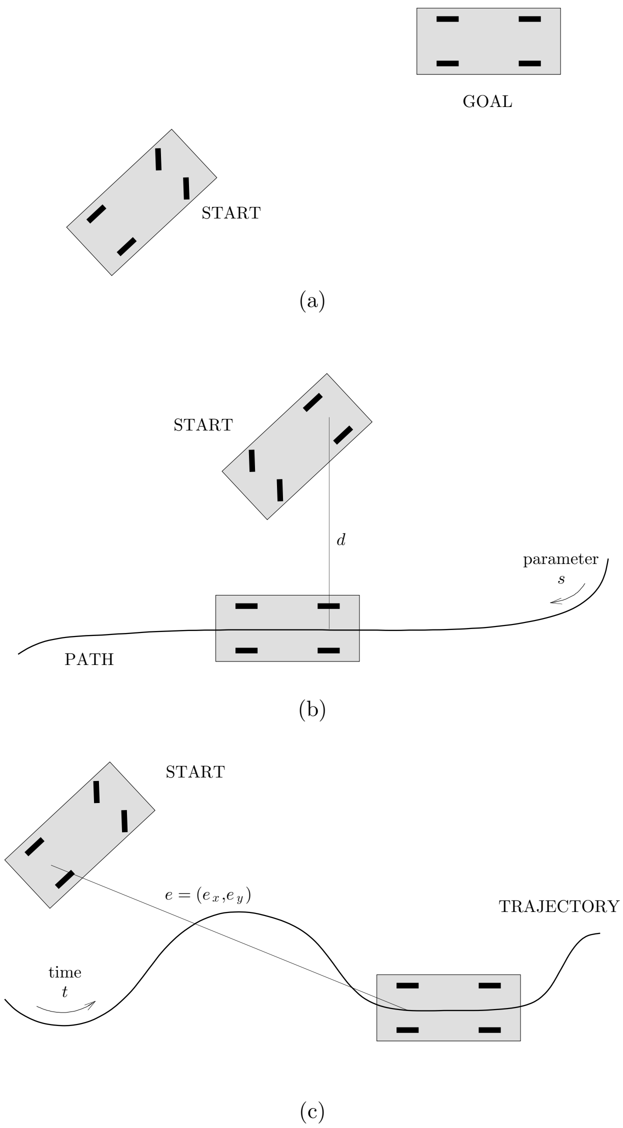

Figure 1: Motion tasks: Point-to-point motion (a), Path following (b), Trajectory tracking (c)

appropriate motion timing. For example, paths with discontinuous curvature (like the Reeds and Shepp optimal paths under maximum curvature constraint) can be executed by the real axle midpoint of a car-like vehicle provided that the robot is allowed to stop, whereas paths with discontinuous tangent are not feasible. In this analysis, the selection of the robot representative point for path/trajectory planning is critical.

The timing profile is the additional item needed in trajectory tracking control tasks. This information is seldom provided by current motion planners, also because the actual dynamics of the specific robot are typically neglected at this level. The above example suggests that it may be reasonable to enforce already at the planning stage requirements such as 'move slower where the path curvature is higher'.

1.2 Control issues

From a control point of view, the previously described motion tasks are defined for the nonlinear system

$$\dot{q} = G(q)v, \tag{1}$$

representing the kinematic model of the robot. Here, q is the n-vector of robot generalized coordinates, v is the m-vector of input velocities ($m < n$), and the columns g_i ($i = 1, \ldots, m$) of matrix G are smooth vector fields. For the car-like robot, it is $n = 4$ and $m = 2$.

The above model can be directly derived from the nonintegrable rolling constraints governing the system kinematic behavior. System (1) is driftless, a characteristic of first-order kinematic models. Besides, its nonlinear nature is intrinsically related to the nonholonomy of the original Pfaffian constraints. In turn, it can be shown that this is equivalent to the global accessibility of the n-dimensional robot configuration space—in spite of the reduced number of inputs.

Interestingly, the nonholonomy of system (1) reverses the usual order of difficulty of robot control tasks. For articulated manipulators, and in general for all mechanical systems with as many control inputs as generalized coordinates, stabilization to a fixed configuration is simpler than tracking a trajectory. Instead, stabilizing a wheeled mobile robot to a point is more difficult than path following or trajectory tracking.

A simple way to appreciate such a difference follows from the general discussion of the previous section. The point-to-point task is actually an input-state problem with $m = 2$ inputs and n controlled states. The path following task is an input-output problem with $m = 1$ input and $p = 1$ controlled output, implying the indirect control of $n - 1$ states. The trajectory tracking task is again an input-output problem with $m = 2$ inputs and $p = 2$ controlled outputs, implying the indirect control of n states. As a result, the point-to-point motion task gives rise to the most difficult control problem, since we are trying to control n independent variables using only two input commands. The path following and trajectory tracking tasks have a similar level of difficulty, being 'square' control problems (same number of control inputs and controlled variables).

This conclusion can be supported by a more rigorous controllability analysis. In particular, one can test whether the above problems admit an approximate solution in terms of linear control design techniques. We shall see that if the system (1) is linearized at a fixed configuration, the resulting linear system is not controllable. On the other hand, the linearization of eq. (1) about a smooth trajectory gives rise to a linear time-varying system that is controllable, provided some persistency conditions are satisfied by the reference trajectory.

The search for a feedback solution to the point stabilization problem is further complicated by a general theoretical obstruction. Although the kinematic model (1) can be shown to be controllable using nonlinear tools from differential geometry, it fails to satisfy a necessary condition for stabilizability via smooth time-invariant feedback (Brockett's theorem). This means that the class of stabilizing controllers should be suitably enlarged so as to include nonsmooth and/or time-varying feedback control laws.

We finally point out that the design of feedback controllers for the path following task can be tackled from two opposite directions. In fact, by separating the geometric and timing information of a trajectory, path following may be seen as a subproblem of trajectory tracking. On the other hand, looking at the problem from the point of view of controlled states (in the proper coordinates), path following appears as part of a point stabilization task. The latter philosophy will be adopted in this chapter.

1.3 Open-loop vs. closed-loop control

Some comments are now appropriate concerning the relationships between the planning and control phases in robot motion execution.

Essentially, we regard planning and open-loop (or feedforward) control as synonyms, as opposed to feedback control. In a general setting, a closed-loop controller results from the superposition of a feedback action to a coherent feedforward term. The latter is determined based on a priori knowledge about the motion task and the environment, which may have been previously acquired by exteroceptive sensors. Feedback control is instead computed in real-time based on external/internal sensor data.

However, the borderline between open-loop and closed-loop control solutions may not be so sharp. In fact, we may use repeated open-loop phases, replanned at higher rates using new sensor data to gather information on the actual state. In the limit, continuous sensing and replanning leads to a feedback solution. Although this scheme is conceptually simple, its convergence analysis may not be easy. Thus, we prefer to consider the planning and control phases separately.

For wheeled mobile robots, the usual output of the planning phase, which takes into account the obstacle avoidance requirement, is a kinematically feasible path with associated nominal open-loop commands. To guarantee feasibility, the planner may either take directly into account the nonholonomic constraints in the generation of a path, or create a preliminary holonomic path with standard techniques and then approximate it with a concatenation of feasible subpaths.

In the planning phase, it is also possible to include an optimality criterion together with system state and input constraints. It is often possible to obtain a solution by applying optimal (open-loop) control results. A typical cost criterion for the car-like robot is the total length of the collision-free path joining source to destination, while constraints include bounds on the steering angle as well as on the linear and angular velocity. In any case, the resulting commands are computed off-line. Hence, unmodeled events at running time, such as occasional slipping of the wheels or erroneous initial localization, will prevent the successful completion of a point-to-point motion or the correct tracing of a desired path.

The well-known answer to such problems is resorting to a feedback controller, driven by the current task error, so as to achieve some degree of robustness. However, this should by no means imply the abdication to the use of the nominal open-loop command computed in the planning phase, which is included as the feedforward term in the closed-loop controller. As soon as the task error is zero, the feedback signal is not in action and the output command of the controller coincides with the feedforward term.

The path and trajectory tracking controllers presented in this chapter agree with this combined approach. In fact, the feedforward represents the anticipative action needed to drive the robot along the desired nominal motion. We point out that a shortcoming arises when the planner generates optimal feedforward commands that are at their saturation level, because this leaves no room for the correcting feedback action. This is a common problem in open-loop optimal control; unfortunately, optimal feedback control laws for nonlinear systems are quite difficult to obtain in explicit form.

On the other hand, it follows from the discussion in Sect. 1.1 that no feedforward is required in principle for the point stabilization task, so that the executed trajectory results from the feedback action alone. While this approach may be satisfactory for fine motion tasks, in gross motion a pure feedback control may drive the mobile robot toward the goal in an unpredictable way. In this case, a closer integration of planning and control would certainly improve the overall performance.

1.4 Organization of contents

We will present some of the most significant feedback control strategies for the different robot motion tasks. For each method, we discuss the single design steps and illustrate the typical performance by simulations. Results are presented in a consistent way in order to allow for comparisons. The organization of the rest of the chapter is as follows.

Section 2 is devoted to preliminary material. The kinematic model of the car-like robot is introduced, stating the main assumptions and distinguishing the cases of rear-wheel and front-wheel driving. We analyze the local controllability properties at a configuration and about a trajectory. Global controllability is proved in a nonlinear setting and a negative result concerning smooth feedback stabilizability is recalled. This section is concluded by presenting the chained-form transformation of the model and its essential features.

In Sect. 3 we address the trajectory tracking problem. The generation of suitable feedforward commands for a given smooth trajectory is discussed. In particular, we point out how geometric and timing information can be handled separately. A simple linear controller is devised for the chained-form representation of the car-like robot, using the approximate system linearization around the nominal trajectory. Then, we present two nonlinear controllers based on exact feedback linearization. The first uses static feedback to achieve input-output linearization for the original kinematic model of the car-like robot. The second is a full-state linearizing dynamic feedback designed on the chained-form representation. Both guarantee global tracking with prescribed linear error dynamics.

In Sect. 4 two time-varying feedback control laws are presented, both solving the point stabilization as well as the path following problem. The two controllers are globally defined on chained-form representations. The first is a smooth time-varying controller based on a Lyapunov analysis of skew-symmetric forms. The second is a nonsmooth time-varying feedback controller inspired by the backstepping approach. Convergence rates of the two methods are discussed and illustrated by simulations.

Section 5 summarizes the obtained results and indicates some possible extensions of the control problem to address the limitations arising in real-world problems.

In the exposition, we shall limit the references only to the basic sources from which the presented material is drawn. In the concluding section, however, a reasoned guide to further related literature is given.

2 Modeling and Analysis of the Car-like Robot

In this section, we shall first derive the kinematic equations of a car-like robot and then analyze the fundamental properties of the corresponding system from a control viewpoint.

2.1 Kinematic modeling

The main feature of the kinematic model of wheeled mobile robots is the presence of nonholonomic constraints due to the *rolling without slipping* condition between the wheels and the ground. The case of a single wheel is analyzed first.

Consider a wheel that rolls on a plane while keeping its body vertical, as shown in Fig. 2. This kind of system is also referred to as a *unicycle*. Its configuration can be described by a vector q of three generalized coordinates, namely the position coordinates x, y of the point of contact with the ground in a fixed frame and the angle θ measuring the wheel orientation with respect to the x axis. The system generalized velocities $\dot{q}$ cannot assume independent values; in particular, they must satisfy the constraint

$$\begin{bmatrix} \sin\theta & -\cos\theta & 0 \end{bmatrix} \begin{bmatrix} \dot{x} \\ \dot{y} \\ \dot{\theta} \end{bmatrix} = 0, \tag{2}$$

entailing that the linear velocity of the wheel center lies in the body plane of the wheel (zero lateral velocity).

Equation (2) is a typical example of *Pfaffian* constraint $C(q)\dot{q} = 0$, i.e., linear in the generalized velocities. As a consequence, all admissible generalized velocities are contained in the null space of the constraint matrix $C(q)$. In this case, one obtains

$$\dot{q} = \begin{bmatrix} \cos\theta \\ \sin\theta \\ 0 \end{bmatrix} v_1 + \begin{bmatrix} 0 \\ 0 \\ 1 \end{bmatrix} v_2, \tag{3}$$

where v_1 and v_2 are respectively the linear velocity of the wheel and its angular velocity around the vertical axis. As the choice of a basis for the null space of matrix C is not unique, the components of v may also assume different meanings.

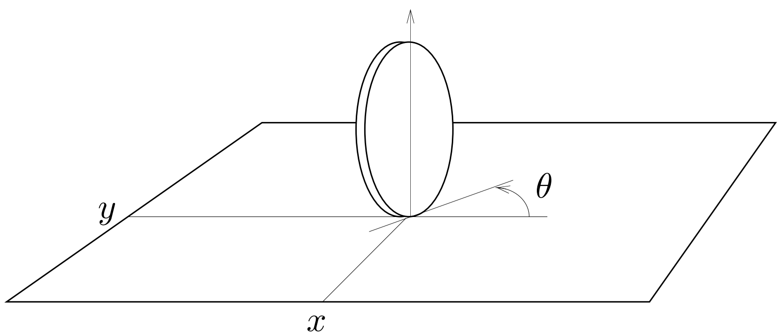

Figure 2: Generalized coordinates of a unicycle

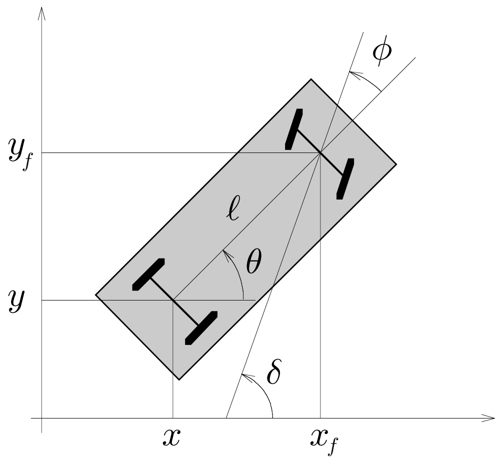

Figure 3: Generalized coordinates of a car-like robot

Moreover, they may have no direct relationship with the actual controls available, that are in general forces or torques. For this reason, eq. (3) is called the *kinematic model* of the unicycle.

Let us now turn to a robot having the same kinematics of an automobile, as shown in Fig. 3. For simplicity, assume that the two wheels on each axle (front and rear) collapse into a single wheel located at the midpoint of the axle (*car-like* model). The front wheel can be steered while the rear wheel orientation is fixed. The generalized coordinates are $q = (x, y, \theta, \phi)$, where x, y are the cartesian coordinates of the rear wheel, θ measures the orientation of the car body with respect to the x axis, and ϕ is the steering angle.

The system is subject to two nonholonomic constraints, one for each wheel:

$$\begin{aligned} \dot{x}_f \sin(\theta + \phi) - \dot{y}_f \cos(\theta + \phi) &= 0 \\ \dot{x} \sin\theta - \dot{y} \cos\theta &= 0, \end{aligned}$$

with x_f, y_f denoting the cartesian coordinates of the front wheel. By using the rigid-body constraint

$$\begin{aligned} x_f &= x + \ell \cos\theta \\ y_f &= y + \ell \sin\theta, \end{aligned}$$

where ℓ is the distance between the wheels, the first kinematic constraint becomes

$$\dot{x} \sin(\theta + \phi) - \dot{y} \cos(\theta + \phi) - \dot{\theta}\, \ell \cos\phi = 0.$$

The Pfaffian constraint matrix is

$$C(q) = \begin{bmatrix} \sin(\theta+\phi) & -\cos(\theta+\phi) & -\ell\cos\phi & 0 \\ \sin\theta & -\cos\theta & 0 & 0 \end{bmatrix},$$

and has constant rank equal to 2.

If the car has *rear-wheel driving*, the kinematic model is derived as

$$\begin{bmatrix} \dot{x} \\ \dot{y} \\ \dot{\theta} \\ \dot{\phi} \end{bmatrix} = \begin{bmatrix} \cos\theta \\ \sin\theta \\ \tan\phi/\ell \\ 0 \end{bmatrix} v_1 + \begin{bmatrix} 0 \\ 0 \\ 0 \\ 1 \end{bmatrix} v_2, \tag{4}$$

where v_1 and v_2 are the *driving* and the *steering* velocity input, respectively. There is a model singularity at $\phi = \pm\pi/2$, where the first vector field has a discontinuity. This corresponds to the car becoming jammed when the front wheel is normal to the longitudinal axis of the body. However, the importance of this singularity is limited, due to the restricted range of the steering angle ϕ in most practical cases.

The model for *front-wheel driving* is obtained as

$$\begin{bmatrix} \dot{x} \\ \dot{y} \\ \dot{\theta} \\ \dot{\phi} \end{bmatrix} = \begin{bmatrix} \cos\theta\cos\phi \\ \sin\theta\cos\phi \\ \sin\phi/\ell \\ 0 \end{bmatrix} v_1 + \begin{bmatrix} 0 \\ 0 \\ 0 \\ 1 \end{bmatrix} v_2,$$

where the driving velocity v_1 refers now to the front wheel. Note that the previous singularity does not occur in this model; in fact, at $\phi = \pm\pi/2$ the car can still (in principle) pivot about its rear wheel.

An interesting format for the kinematic equations of a front-wheel drive car can be obtained by means of a change of coordinates and an input transformation. In particular, define the alternative set of generalized coordinates $(x_f, y_f, \delta, \theta)$, where $\delta = \theta + \phi$ is the *absolute* steering angle with respect to the x-axis (see Fig. 3). By using the input transformation

$$\begin{aligned} w_1 &= v_1 \\ w_2 &= \frac{1}{\ell}\sin(\delta-\theta)v_1 + v_2, \end{aligned}$$

it is easy to show that

$$\begin{bmatrix} \dot{x}_f \\ \dot{y}_f \\ \dot{\delta} \\ \dot{\theta} \end{bmatrix} = \begin{bmatrix} \cos\delta \\ \sin\delta \\ 0 \\ \sin(\delta-\theta)/\ell \end{bmatrix} w_1 + \begin{bmatrix} 0 \\ 0 \\ 1 \\ 0 \end{bmatrix} w_2.$$

Note that the first three equations are those of a unicycle. As a matter of fact, the above model is equivalent to a unicycle with one trailer hooked at the center of the wheel. Correspondingly, the new input w_2 is the absolute (i.e., measured w.r.t. the x axis) steering velocity of the front wheel. Other state and input transformations of the car-like kinematics will be presented in Sect. 2.3.

Throughout the rest of this chapter, we shall be dealing with the rear-wheel drive model (4). It has to be mentioned that a more complete kinematic model should include also the rotation angles of each wheel as generalized coordinates, in order to account for the presence of actuators and sensors on the wheel axis as well as for typical nonidealities such as tire deformation. Nevertheless, our model captures the essence of the vehicle kinematics and is well suited for control purposes.

2.2 Controllability analysis

Equation (4) may be rewritten as

$$\dot{q} = g_1(q)v_1 + g_2(q)v_2, \qquad \text{with} \quad g_1 = \begin{bmatrix} \cos\theta \\ \sin\theta \\ \tan\phi/\ell \\ 0 \end{bmatrix}, \; g_2 = \begin{bmatrix} 0 \\ 0 \\ 0 \\ 1 \end{bmatrix}. \tag{5}$$

The above system is nonlinear, driftless (i.e., no motion takes place under zero input) and there are less control inputs than generalized coordinates.

Although any driver's experience indicates that a car-like robot should be completely controllable, it is not trivial to establish such property on a mathematical basis. In particular, we shall see that an approximate linear analysis is not sufficient in general to achieve this goal.

2.2.1 Controllability at a point

As system (5) is driftless, any configuration q_e is an equilibrium point under zero input. The easiest way to investigate its controllability at q_e is to consider the corresponding linear approximation

$$\dot{\tilde{q}} = g_1(q_e)v_1 + g_2(q_e)v_2 = G(q_e)v,$$

where $\tilde{q} = q - q_e$. The rank of the controllability matrix $G(q_e)$ is two. Hence, the linearized system is not controllable so that a linear controller will not work, not even locally.

A useful tool that allows to test the controllability of driftless nonlinear systems is the *Lie Algebra rank condition* [18]. In our case, this boils down to check whether

$$\text{rank}\,[g_1 \;\; g_2 \;\; [g_1, g_2] \;\; [g_1, [g_1, g_2]] \;\; [g_2, [g_1, g_2]] \ldots \;\;] = 4.$$

For system (5), the first two Lie brackets are computed as

$$[g_1, g_2] = \begin{bmatrix} 0 \\ 0 \\ -1/\ell\cos^2\phi \\ 0 \end{bmatrix}, \qquad [g_1, [g_1, g_2]] = \begin{bmatrix} -\sin\theta/\ell\cos^2\phi \\ \cos\theta/\ell\cos^2\phi \\ 0 \\ 0 \end{bmatrix}.$$

It is easy to verify that, away from the model singularity $\phi = \pm\pi/2$, the above rank is 4, so that the car-like robot is certainly controllable whenever the steering angle is different from $\pm\pi/2$. Using the fact that ϕ can be modified at will through the control input v_2, it can be shown that the system is actually controllable everywhere.

As for the stabilizability of system (5), the failure of the previous linear analysis indicates that exponential stability in the sense of Lyapunov cannot be achieved by smooth feedback [45]. However, things turn out to be even worse: it is not possible to stabilize at all the system at q_e by using a smooth (in fact, continuous) time-invariant feedback law $v = v(q)$. This negative result can be readily established on the basis of Brockett's theorem [6], which implies that a necessary condition for smooth stabilizability of a driftless *regular* system (i.e., such that the input vector fields are linearly independent at q_e) is that the number of inputs equals the number of states. Since this is not the case, such condition is violated.

The above limitation has a deep impact on the control design approach. To obtain a point stabilizing controller it is either necessary to give up the continuity requirement, or to resort to time-varying control laws $v = v(q, t)$. In Sect. 4 we shall pursue the latter approach.

2.2.2 Controllability about a trajectory

Consider now a desired reference state trajectory $q_d(t) = (x_d(t), y_d(t), \theta_d(t), \phi_d(t))$ for the car-like robot. In order to be feasible, this trajectory must satisfy the non-holonomic constraints on the vehicle motion. The generation of such trajectories as well as of the corresponding reference velocity inputs v_{d1} and v_{d2} will be addressed in Sect. 3.

Defining $\tilde{q}(t) = q(t) - q_d(t)$ and $\tilde{v}(t) = v(t) - v_d(t)$, the approximate linearization of system (5) about the reference trajectory is obtained as

$$\dot{\tilde{q}} = A(t)\tilde{q} + B(t)\tilde{v}, \tag{6}$$

with

$$A(t) = \sum_{i=1}^{2} v_{di}(t) \left.\frac{\partial g_i}{\partial q}\right|_{q=q_d(t)}, \qquad B(t) = G(q_d(t)).$$

Simple computations yield

$$A(t) = \begin{bmatrix} 0 & 0 & -\sin\theta_d(t)v_{d1}(t) & 0 \\ 0 & 0 & \cos\theta_d(t)v_{d1}(t) & 0 \\ 0 & 0 & 0 & v_{d1}(t)/\ell\cos^2\theta_d(t) \\ 0 & 0 & 0 & 0 \end{bmatrix}, \quad B(t) = \begin{bmatrix} \cos\theta_d(t) & 0 \\ \sin\theta_d(t) & 0 \\ \tan\theta_d(t)/\ell & 0 \\ 0 & 1 \end{bmatrix}.$$

Note that the linearized system is *time-varying* through the dependence on time of the reference trajectory. As a consequence, the controllability analysis is more involved than in the time-invariant case, and would consist in testing whether the *controllability Gramian* is nonsingular [19].

For illustration, we consider the special case of a linear trajectory with constant velocity, in which one falls upon a time-invariant system. In fact, in this situation we have $v_{d1}(t) \equiv v_{d1}$ (a constant nonzero value) and $v_{d2}(t) \equiv 0$. Besides, $\theta_d(t) \equiv \theta_d(t_0)$ and $\phi(t) \equiv 0$. The controllability condition is

$$\text{rank}\left[B \ \ AB \ \ A^2B \ \ A^3B\right] = 4.$$

It is easy to verify that the controllability matrix has a single nonzero 4×4 minor whose value is $-u_{d1}^3/\ell^2\cos^4\theta_d$. Therefore, the linearized system is controllable as long as $\theta_d \neq \pm\pi/2$ and $u_{d1} \neq 0$ (which is not unexpected, since for $u_{d1} = 0$ the trajectory would collapse to a point). This implies that system (5) can be locally stabilized about the reference trajectory by a linear feedback.

Although the above analysis has been carried out for a linear reference trajectory, we shall see in Sect. 3 that it is possible to design a locally stabilizing linear feedback for arbitrary feasible trajectories provided they do not come to a stop.

2.3 Chained forms

The existence of canonical forms for kinematic models of nonholonomic robots is essential for the systematic development of both open-loop and closed-loop control strategies. The most useful canonical structure is the *chained form.*

The two-input driftless control system

$$\begin{aligned} \dot{x}_1 &= u_1 \\ \dot{x}_2 &= u_2 \\ \dot{x}_3 &= x_2u_1 \\ &\vdots \\ \dot{x}_n &= x_{n-1}u_1, \end{aligned} \tag{7}$$

is called $(2, n)$ single-chain form [28]. The two-input case covers many of the kinematic models of practical wheeled mobile robots. A more general study would involve multiple chains, with rather straightforward extensions of the results presented in this chapter.

The chained system (7), although nonlinear, has a strong underlying linear structure. This clearly appears when u_1 is assigned as a function of time, and is no longer regarded as a control variable. In this case, eq. (7) becomes a single-input, time-varying linear system.

The $(2, n)$ chained form can be shown to be completely controllable by application of the Lie Algebra rank condition. In performing this calculation, one finds that all Lie brackets above a certain order (namely, $n-2$) are identically zero; this property of the system is called *nilpotency*.

Necessary and sufficient conditions have been given in [29] for the conversion of a two-input system like (5) into chained form by means of *(i)* a change of coordinates $x = \phi(q)$, and *(ii)* an invertible input transformation $v = \beta(q)u$. By applying these conditions, one can show that nonholonomic systems with $m = 2$ inputs and $n = 3$ or 4 generalized coordinates can be always put in chained form.

For example, consider the kinematic model (3) of a unicycle. By letting

$$\begin{aligned} x_1 &= -\theta \\ x_2 &= x\cos\theta + y\sin\theta \\ x_3 &= -x\sin\theta + y\cos\theta, \end{aligned}$$

and

$$\begin{aligned} v_1 &= x_3 u_1 + u_2 = (-x\sin\theta + y\cos\theta)u_1 + u_2 \\ v_2 &= -u_1, \end{aligned}$$

it is easy to see that the transformed system is in (2,3) chained form. Besides, both the coordinate and the input transformation are globally defined. Note that the new variables x_2 and x_3 are simply the cartesian coordinates of the unicycle evaluated in the mobile frame attached to the robot body and rotated so as to align the x_2 axis with the vehicle orientation.

Let us now consider the car-like robot model (5). Using the change of coordinates

$$\begin{aligned} x_1 &= x \\ x_2 &= \tan\phi/\ell\cos^3\theta \\ x_3 &= \tan\theta \\ x_4 &= y, \end{aligned} \tag{8}$$

together with the input transformation

$$\begin{aligned} v_1 &= u_1/\cos\theta \\ v_2 &= -3\sin\theta\sin^2\phi\, u_1/\ell\cos^2\theta + \ell\cos^3\theta\cos^2\phi\, u_2, \end{aligned} \tag{9}$$

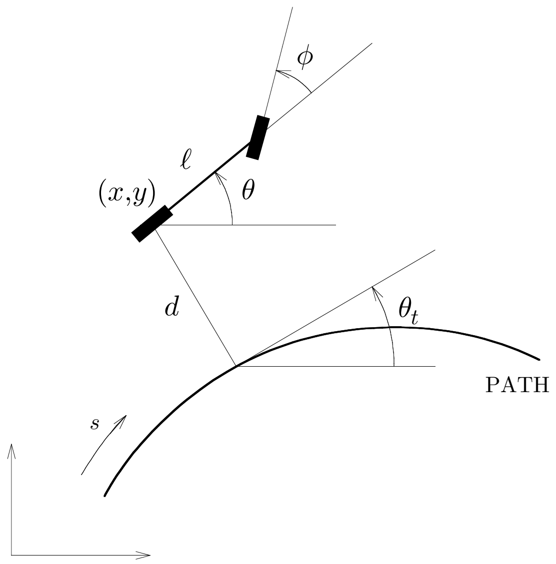

Figure 4: Coordinate definition for a path following task

the system is in $(2,4)$ chained form

$$\begin{aligned} \dot{x}_1 &= u_1 \\ \dot{x}_2 &= u_2 \\ \dot{x}_3 &= x_2 u_1 \\ \dot{x}_4 &= x_3 u_1. \end{aligned} \tag{10}$$

In this case, the transformation (and thus, the obtained chained form) is only locally defined in open connected domains which exclude the vehicle orientations $\theta = \pi/2 \pm k\pi$, $k \in I\!N$. The structure of change of coordinates (8) is interesting because it can be generalized to nonholonomic systems of higher dimension, such as the N-trailer robot [46]. In particular, the x_1 and x_n coordinates can be always chosen as the x and y coordinates of the midpoint of the last trailer wheel axle.

It is interesting to note that the $(2,n)$ chained form can be also obtained starting from a different point of view. In particular, assume that the car-like robot must follow a given path which is parameterized by its arc length. With reference to Fig. 4, let d be the distance between the rear axle midpoint and the path, and s be the corresponding value of the path parameter. Denote by θ_t the angle between the current tangent to the path and the x axis, and let $\theta_p = \theta - \theta_t$. The curvature along the path is defined as

$$c(s) = \frac{d\theta_t}{ds},$$

which implies

$$\dot{\theta}_t = c(s)\dot{s}. \tag{11}$$

In the following, we assume that $c(\cdot) \in C^1$ and that the path satisfies some technical conditions (see [44] for details). It is easy to verify that

$$\begin{aligned} \dot{s} &= v_1 \cos\theta_p + \dot{\theta}_t\, d && (12)\\ \dot{d} &= v_1 \sin\theta_p. && (13) \end{aligned}$$

Equations (12–13) may be combined with model (4) in order to derive the kinematic equations in terms of *path coordinates* $q_p = (s, d, \theta_p, \phi)$:

$$\begin{bmatrix} \dot{s} \\ \dot{d} \\ \dot{\theta}_p \\ \dot{\phi} \end{bmatrix} = \begin{bmatrix} \dfrac{\cos\theta_p}{1 - dc(s)} \\ \sin\theta_p \\ \left(\dfrac{\tan\phi}{\ell} - \dfrac{c(s)\cos\theta_p}{1 - dc(s)}\right) \\ 0 \end{bmatrix} v_1 + \begin{bmatrix} 0 \\ 0 \\ 0 \\ 1 \end{bmatrix} v_2. \tag{14}$$

The above model can be put in the $(2, 4)$ chained form by using the change of coordinates

$$\begin{aligned} x_1 &= s \\ x_2 &= -c'(s) d \tan\theta_p - c(s)(1 - dc(s)) \frac{1 + \sin^2\theta_p}{\cos^2\theta_p} + \frac{(1 - dc(s))^2 \tan\phi}{\ell \cos^3\theta_p} \\ x_3 &= (1 - dc(s)) \tan\theta_p \\ x_4 &= d, \end{aligned} \tag{15}$$

together with the input transformation

$$\begin{aligned} v_1 &= \frac{1 - dc(s)}{\cos\theta_p} u_1 \\ v_2 &= \alpha_2(q_p)(u_2 - \alpha_1(q_p) u_1). \end{aligned}$$

In the above formulas, $c'(s)$ denotes the derivative of c with respect to s, and we have set

$$\begin{aligned} \alpha_1(q_p) &= \frac{\partial x_2}{\partial s} + \frac{\partial x_2}{\partial d}(1 - dc(s)) \tan\theta_p + \frac{\partial x_2}{\partial \theta_p}\left(\frac{\tan\phi\,(1 - dc(s))}{\ell \cos\theta_p} - c(s)\right) \\ \alpha_2(q_p) &= \frac{\ell \cos^3\theta_p \cos^2\phi}{(1 - dc(s))^2}. \end{aligned}$$

Also this chained-form transformation is locally defined in open connected domains, because $\theta_p = \pi/2 \pm k\pi$, $k \in \mathbb{N}$, must be excluded. Note that in the particular case

$c(s) \equiv 0$, one recovers the previous expressions (8) and (9). In fact, in this situation the path may be taken as the x-axis of the world frame, and (s, d, θ_p) become the coordinates (x, y, θ) of the vehicle.

We conclude this section by pointing out that there are other canonical forms that can be successfully used in connection with nonholonomic systems, namely the *Čaplygin form* and the *power form*. It is noteworthy that, for $m = 2$ inputs, the three canonical forms are mathematically equivalent, since there exist global coordinate transformations that allow to convert one into the others [21].

3 Trajectory Tracking

In this section, we consider the problem of tracking a given cartesian trajectory with the car-like robot using feedback control. Both a local and a global approach will be presented. In the first, we use a standard linear control design and obtain convergence provided that the car starts sufficiently close to the desired trajectory. In the second, we pursue a feedback linearization approach, achieving asymptotic stability for arbitrary initial states via static as well as dynamic nonlinear feedback.

In the following, extensive use is made of the chained-form representation. Such system transformation is not strictly necessary, but simplifies considerably the control design and provides at the same time a framework for the direct extension of the controllers to vehicles with more complex kinematics. In any case, the methods presented here can be applied to more general mobile robots, even those which cannot be put in chained form.

Before moving to the control design, we discuss the problem of generating state reference trajectories for the car-like robot, both in the original kinematic description (5) and in the chained form (10).

3.1 Reference trajectory generation

Assume that a feasible and smooth desired *output trajectory* is given in terms of the cartesian position of the car rear wheel, i.e.,

$$x_d = x_d(t), \quad y_d = y_d(t), \qquad t \geq t_0. \tag{16}$$

This natural way of specifying the motion of a car-like robot has an appealing property. In fact, from this information we are able to derive the corresponding time evolution of the remaining coordinates (*state trajectory*) as well as of the associated input commands (*input trajectory*) as shown hereafter.

The desired output trajectory (16) is feasible when it can be obtained from the evolution of a reference car-like robot

$$\begin{aligned} \dot{x}_d &= \cos\theta_d \, v_{d1} && (17)\\ \dot{y}_d &= \sin\theta_d \, v_{d1} && (18)\\ \dot{\theta}_d &= \tan\phi_d \, v_{d1}/\ell && (19)\\ \dot{\phi}_d &= v_{d2}, && (20) \end{aligned}$$

for suitable initial conditions $(x_d(t_0), y_d(t_0), \theta_d(t_0), \phi_d(t_0))$ and piecewise-continuous inputs $v_d(t)$, for $t \geq t_0$.

Solving for v_{d1} from eqs. (17) and (18) gives for the first input

$$v_{d1}(t) = \pm\sqrt{\dot{x}_d^2(t) + \dot{y}_d^2(t)}, \tag{21}$$

where the sign depends on the choice of executing the trajectory with forward or backward car motion, respectively.

Dividing eq. (18) by (17), and keeping the sign of the linear velocity input into account, we compute the desired orientation of the car as

$$\theta_d(t) = \mathrm{ATAN2}\left\{\frac{\dot{y}_d(t)}{v_{d1}(t)}, \frac{\dot{x}_d(t)}{v_{d1}(t)}\right\}, \tag{22}$$

with codomain in all four quadrants.

Differentiating eqs. (17) and (18), and combining the results so as to eliminate $\dot{v}_{d1}$, we obtain

$$\dot{\theta}_d(t) = \frac{\ddot{y}_d(t)\dot{x}_d(t) - \ddot{x}_d(t)\dot{y}_d(t)}{v_{d1}^2(t)}.$$

Plugging this into eq. (19) provides the desired steering angle

$$\phi_d(t) = \arctan\frac{\ell\left[\ddot{y}_d(t)\dot{x}_d(t) - \ddot{x}_d(t)\dot{y}_d(t)\right]}{v_{d1}^3(t)}, \tag{23}$$

which takes values in $(-\pi/2, \pi/2)$.

Finally, differentiating (23) and substituting the result in eq. (20) yields the second input

$$v_{d2}(t) = \ell v_{d1}\,\frac{(\ddot{y}_d\dot{x}_d - \ddot{x}_d\dot{y}_d)\,v_{d1}^2 - 3\,(\ddot{y}_d\dot{x}_d - \ddot{x}_d\dot{y}_d)\,(\dot{x}_d\ddot{x}_d + \dot{y}_d\ddot{y}_d)}{v_{d1}^6 + \ell^2\,(\ddot{y}_d\dot{x}_d - \ddot{x}_d\dot{y}_d)^2}, \tag{24}$$

where we dropped for compactness the time dependence in the right hand side.

Equations (21–24) provide the *unique* state and input trajectory (modulo the choice of forward or backward motion) needed to reproduce the desired output trajectory. These expressions depend only on the values of the output trajectory (16) and its derivatives up to the third order. Therefore, in order to guarantee its exact reproducibility, the cartesian trajectory should be three times differentiable almost everywhere. This fact should be taken into account at the motion planning level.

For illustration, consider a circular trajectory of radius R to be traced counterclockwise at a constant linear velocity $R\omega$, with the rear wheel of the car located at the origin at time $t_0 = 0$. We have

$$x_d(t) = R \sin \omega t, \qquad y_d(t) = R(1 - \cos \omega t).$$

From the previous formulas, when the robot is required to move in the forward direction, the nominal command inputs are computed as

$$v_{d1}(t) = R\omega, \qquad v_{d2}(t) = 0,$$

while the unique initial state enabling exact reproduction of the desired trajectory is

$$x_d(0) = 0, \quad y_d(0) = 0, \quad \theta_d(0) = 0, \quad \phi_d(0) = \arctan \frac{\ell}{R}.$$

The only situation in which the reference signals (21–24) are not defined is when $v_{d1}(\bar{t}) = 0$ for some $\bar{t} \geq t_0$. In this case, it is convenient to use a parameterized trajectory in which the geometric path description is separated from the timing information. Denoting by σ the path parameter (e.g., the arc length s) and by $\sigma = \sigma(t)$ the time history along the trajectory, one has

$$\dot{x}_d(t) = \frac{d}{d\sigma} x_d(\sigma) \cdot \frac{d\sigma}{dt} = x'_d(\sigma(t))\dot{\sigma}(t)$$

and a similar expression for $\dot{y}_d(t)$ (the prime denotes differentiation with respect to the path parameter). We can then rewrite the linear pseudo-velocity command at a given point on the path as

$$w_{d1}(\sigma) = \pm\sqrt{{x'_d}^2(\sigma) + {y'_d}^2(\sigma)}. \tag{25}$$

The actual linear velocity input is expressed as

$$v_{d1}(t) = w_{d1}(\sigma(t))\dot{\sigma}(t).$$

The situation $v_{d1}(\bar{t}) = 0$ is then obtained by letting $\dot{\sigma}(\bar{t}) = 0$, with $w_{d1}(\sigma(\bar{t})) \neq 0$.

The desired orientation is computed as

$$\theta_d(\sigma) = \mathrm{ATAN2}\left\{\frac{y'_d(\sigma)}{w_{d1}(\sigma)}, \frac{x'_d(\sigma)}{w_{d1}(\sigma)}\right\},$$

which is now always well defined. By performing the time/space separation also in eqs. (23) and (24), the zero-velocity singularity is similarly avoided, because only curvature and higher-order information about the path appear in the expressions of $\phi_d(\sigma)$ and $w_{d2}(\sigma)$, with $v_{d2}(t) = w_{d2}(\sigma(t))\dot{\sigma}(t)$. We have in fact

$$\phi_d(\sigma) = \arctan \frac{\ell\left(y''_d(\sigma)x'_d(\sigma) - x''_d(\sigma)y'_d(\sigma)\right)}{w^3_{d1}(\sigma)}$$

and

$$w_{d2}(\sigma) = \frac{\ell w_{d1}\left[\left(y'''_d x'_d - x'''_d y'_d\right) - 3\left(y''_d x'_d - x''_d y'_d\right)\left(x'_d x''_d + y'_d y''_d\right)\right)}{w^6_{d1} + \ell^2\left(y''_d x'_d - x''_d y'_d\right)^2},$$

where we dropped the dependence on σ for compactness.

The derivation of the reference inputs that generate a desired cartesian trajectory of the car-like robot can also be performed for the $(2,4)$ chained form. In fact, with the reference system given by

$$\begin{aligned}
\dot{x}_{d1} &= u_{d1} \\
\dot{x}_{d2} &= u_{d2} \\
\dot{x}_{d3} &= x_{d2}u_{d1} \\
\dot{x}_{d4} &= x_{d3}u_{d1},
\end{aligned} \tag{26}$$

from the output trajectory (16) and the change of coordinates (8) we easily obtain

$$\begin{aligned}
x_{d1}(t) &= x_d(t) \\
x_{d2}(t) &= \left[\ddot{y}_d(t)\dot{x}_d(t) - \dot{y}_d(t)\ddot{x}_d(t)\right]/\dot{x}^3_d(t) \\
x_{d3}(t) &= \dot{y}_d(t)/\dot{x}_d(t) \\
x_{d4}(t) &= y_d(t),
\end{aligned}$$

and

$$\begin{aligned}
u_{d1}(t) &= \dot{x}_d(t) \\
u_{d2}(t) &= \left[\dddot{y}_d(t)\dot{x}^2_d(t) - \dddot{x}_d(t)\dot{y}_d(t)\dot{x}_d(t) - 3\ddot{y}_d(t)\dot{x}_d(t)\ddot{x}_d(t) + 3\dot{y}_d(t)\ddot{x}^2_d(t)\right]/\dot{x}^4_d(t).
\end{aligned}$$

To work out an example for this case, consider a sinusoidal trajectory stretching along the x axis and starting from the origin at time $t_0 = 0$

$$x_d(t) = t, \qquad y_d(t) = A\sin\omega t. \tag{27}$$

The feedforward commands for the chained-form representation are given by

$$u_{d1}(t) = 1, \qquad u_{d2}(t) = -A\,\omega^3 \cos\omega t,$$

while its initial state should be set at

$$x_{d1}(0) = 0, \quad x_{d2}(0) = 0, \quad x_{d3}(0) = A\,\omega, \quad x_{d4}(0) = 0.$$

We note that, if the change of coordinates (8) is used, there is an 'asymmetric' singularity in the state and input trajectory when $\dot{x}_d(\bar{t}) = 0$, for some $\bar{t} > t_0$. This coincides with the situation $\theta_d(\bar{t}) = \pi/2$, where the chained-form transformation is not defined.

On the other hand, if the chained form comes from the model in path variables (14) through the change of coordinates (15), the state and input trajectory needed to track the reference output trajectory $s = s_d(t)$, $d = d_d(t) = 0$, $t \geq t_0$, are simply obtained as

$$\begin{aligned}
x_{d1}(t) &= s_d(t) \\
x_{d2}(t) &= 0 \\
x_{d3}(t) &= 0 \\
x_{d4}(t) &= 0
\end{aligned}$$

and

$$\begin{aligned}
u_{d1}(t) &= \dot{s}_d(t) \\
u_{d2}(t) &= 0,
\end{aligned}$$

without any singularity.

Similar developments can be repeated more in general, e.g., for the case of a nonholonomic mobile robot with N trailers. In fact, once the position of the last trailer is taken as the system output, it is possible to compute the evolution of the remaining state variables as well as of the system inputs as functions of the output trajectory (i.e., of the output and its derivatives up to a certain order). Not surprisingly, the same is true for the chained form (7) by defining (x_1, x_n) as system outputs.

The above property has been also referred to as *differential flatness* [36], and is mathematically equivalent to the existence of a dynamic state feedback transformation that puts the system into a linear and decoupled form consisting of input-output chains of integrators. The algorithmic implementation of the latter idea will be shown in Sect. 3.3.2.

3.2 Control via approximate linearization

We now present a feedback controller for trajectory tracking based on standard linear control theory. The design makes use of the approximate linearization of the system equations about the desired trajectory, a procedure that leads to a time-varying system as seen in Sect. 2.2.2. A remarkable feature of this approach in the present case is the possibility of assigning a time-invariant eigenstructure to the closed-loop error dynamics.

In order to have a systematic procedure that can be easily extended to higher-dimensional wheeled robots (i.e., $n > 4$), the method is illustrated for the chained form case. However, similar design steps for a mobile robot in original coordinates can be found in [42].

For the chained-form representation (10), denote by $(x_{d1}(t), x_{d2}(t), x_{d3}(t), x_{d4}(t))$ and $u_d(t) = (u_{d1}(t), u_{d2}(t))$ the desired state and input trajectory computed in correspondence to the reference cartesian trajectory as in Sect. 3.1. Denote the state and input errors respectively as

$$\tilde{x}_i = x_{di} - x_i, \quad i = 1, \dots, 4, \qquad \tilde{u}_j = u_{dj} - u_j, \quad j = 1, 2.$$

The nonlinear error equations are

$$\begin{aligned} \dot{\tilde{x}}_1 &= \tilde{u}_1 \\ \dot{\tilde{x}}_2 &= \tilde{u}_2 \\ \dot{\tilde{x}}_3 &= x_{d2}u_{d1} - x_2 u_1 \\ \dot{\tilde{x}}_4 &= x_{d3}u_{d1} - x_3 u_1. \end{aligned}$$

Linearizing about the desired trajectory yields the following linear time-varying system

$$\dot{\tilde{x}} = \begin{bmatrix} 0 & 0 & 0 & 0 \\ 0 & 0 & 0 & 0 \\ 0 & u_{d1}(t) & 0 & 0 \\ 0 & 0 & u_{d1}(t) & 0 \end{bmatrix} \tilde{x} + \begin{bmatrix} 1 & 0 \\ 0 & 1 \\ x_{d2}(t) & 0 \\ x_{d3}(t) & 0 \end{bmatrix} \tilde{u} = A(t)\tilde{x} + B(t)\tilde{u}.$$

This system shares the same controllability properties of eq. (6), which was obtained by linearizing the original robot equations (5) about the desired trajectory. For example, it is easily verified that the controllability rank condition is satisfied along a linear trajectory with constant velocity, which is obtained for $u_{d1}(t) \equiv u_{d1}$ (a constant nonzero value) and $u_{d2}(t) \equiv 0$, implying $x_{d2}(t) \equiv 0$ and $x_{d3}(t) \equiv x_{d3}(t_0)$.

Define the feedback term $\tilde{u}$ as the following linear time-varying law

$$\tilde{u}_1 = -k_1 \tilde{x}_1 \tag{28}$$

$$\tilde{u}_2 = -k_2 \tilde{x}_2 - \frac{k_3}{u_{d1}} \tilde{x}_3 - \frac{k_4}{u_{d1}^2} \tilde{x}_4, \tag{29}$$

with k_1 positive, and k_2, k_3, k_4 such that

$$\lambda^3 + k_2\lambda^2 + k_3\lambda + k_4$$

is a Hurwitz polynomial. With this choice, the closed-loop system matrix

$$A_{cl}(t) = \begin{bmatrix} -k_1 & 0 & 0 & 0 \\ 0 & -k_2 & -k_3/u_{d1}(t) & -k_4/u_{d1}^2(t) \\ -k_1 x_{d2}(t) & u_{d1}(t) & 0 & 0 \\ -k_1 x_{d3}(t) & 0 & u_{d1}(t) & 0 \end{bmatrix}$$

has constant eigenvalues with negative real part. While this does not guarantee in itself [20] asymptotic stability of the closed-loop time-varying system, a sufficient condition is that the eigenvalues of the symmetric matrix $A_{cl} + A_{cl}^T$ are strictly negative, which can be shown to be the case here. This sufficient condition follows from the fact that the derivative of the Lyapunov function $\|\tilde{x}\|^2$ is equal to $\tilde{x}^T \left(A_{cl} + A_{cl}^T \right) \tilde{x}$, and is thus smaller than $\lambda_{\min}\|\tilde{x}\|^2$, being $\lambda_{\min}$ the least negative eigenvalue of $A_{cl} + A_{cl}^T$.

The location of the closed-loop eigenvalues in the open left half-plane may be chosen according to the general principle of obtaining fast convergence to zero of the tracking error with a reasonable control effort. For example, in order to assign two real negative eigenvalues in $-\lambda_1$ and $-\lambda_2$ and two complex eigenvalues with negative real part, modulus ω_n and damping coefficient ζ $(0 < \zeta \leq 1)$, the gains k_i should be selected as

$$k_1 = \lambda_1, \quad k_2 = \lambda_2 + 2\zeta\omega_n, \quad k_3 = \omega_n^2 + 2\zeta\omega_n\lambda_2, \quad k_4 = \omega_n^2\lambda_2.$$

Note that the overall control input to the chained-form representation is

$$u = u_d + \tilde{u},$$

with a feedforward and a feedback component. In order to compute the actual input commands v for the car-like robot, one should use the input transformation (9). As a result, the driving and steering velocity inputs are expressed as nonlinear (and for v_2, also time-varying) feedback laws.

The choice (29) for the second control input requires $u_{d1} \neq 0$. Intuitively, placing the eigenvalues at a constant location will require larger gains as the desired motion of the variable x_1 is coming to a stop. One way to overcome this limitation is to assign the eigenvalues as functions of the input u_{d1}. For example, imposing (beside the eigenvalue in $-\lambda_1$) three coincident real eigenvalues in $-\alpha|u_{d1}|$, with $\alpha > 0$, we obtain

$$\tilde{u}_2 = -3\alpha|u_{d1}|\tilde{x}_2 - 3\alpha^2 u_{d1}\tilde{x}_3 - \alpha^3|u_{d1}|\tilde{x}_4, \tag{30}$$

in place of eq. (29). With this *input scaling* procedure, the second control input simply goes to zero when the desired trajectory x_{d1} stops. This procedure will be used also in Sect. 4.1.1.

3.2.1 Simulation results

The simple controller (28-29) has been simulated for a car-like robot with $\ell = 1$ m tracking the sinusoidal trajectory (27), where $A = 1$ and $\omega = \pi$. The state at $t_0 = 0$ is

$$x_1(0) = -2, \quad x_2(0) = 0, \quad x_3(0) = A\,\omega, \quad x_4(0) = -1,$$

so that the car-like robot is initially off the desired trajectory. We have chosen $\lambda_1 = \lambda_2 = \omega_n = 5$ and $\zeta = 1$, resulting in four coincident closed-loop eigenvalues located at -5.

The obtained results are shown in Figs. 5–7 in terms of tracking errors on the original states x, y, θ and ϕ, and of actual control inputs v_1 and v_2 to the car-like robot. Once convergence is achieved (approximately, after 2.5 sec), the control inputs virtually coincide with the feedforward commands associated to the nominal sinusoidal trajectory, as computed from eqs. (21) and (24).

Since the control design is based on approximate linearization, the controlled system is only locally asymptotically stable. However, extensive simulation shows that, also in view of the chained-form transformation, the region of asymptotic stability is quite large—although its accurate determination may be difficult. As a consequence, the car-like robot converges to the desired trajectory even for large initial errors. The transient behavior, however, may deteriorate in an unacceptable way.

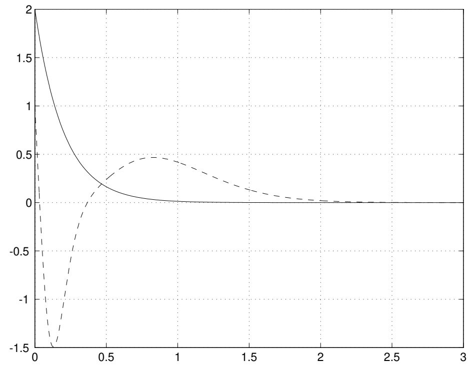

Figure 5: Tracking a sinusoid with approximate linearization: x (—), y (−−) errors (m) vs. time (sec)

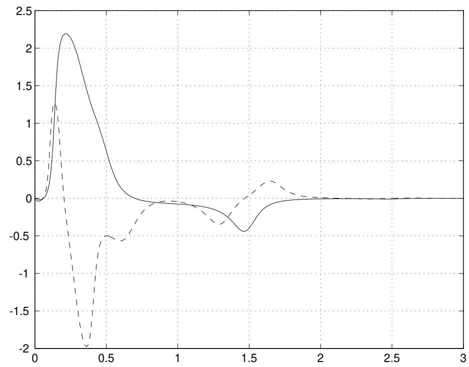

Figure 6: Tracking a sinusoid with approximate linearization: θ (—), ϕ (−−) errors (rad) vs. time (sec)

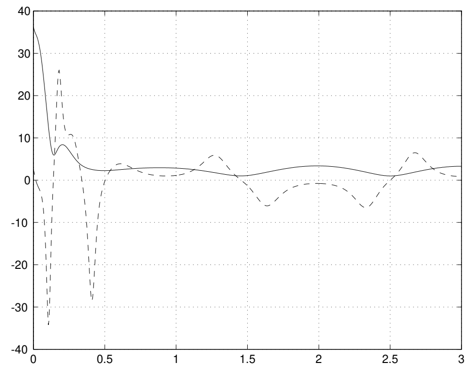

Figure 7: Tracking a sinusoid with approximate linearization: v_1 (—) (m/sec), v_2 (−−) (rad/sec) vs. time (sec)

3.3 Control via exact feedback linearization

We now turn to the use of nonlinear feedback design for achieving global stabilization of the trajectory tracking error to zero.

It is well known in robotics that, if the number of generalized coordinates equals the number of input commands, one can use a nonlinear static (i.e., memoryless) state feedback law in order to transform exactly the nonlinear robot kinematics and/or dynamics into a linear system. In general, the linearity of the system equations is displayed only after a coordinate transformation in the state space. On the linear side of the problem, it is rather straightforward to complete the synthesis of a stabilizing controller. For example, this is the principle of the *computed torque* control method for articulated manipulators.

Actually, two types of exact linearization problems can be considered for a nonlinear system with outputs. Beside the possibility of transforming via feedback the whole set of differential equations into a linear system (*full-state linearization*), one may seek a weaker result in which only the input-output differential map is made linear (*input-output linearization*). Necessary and sufficient conditions exist for the solvability of both problems via static feedback, while only sufficient (but constructive) conditions can be given for the dynamic feedback case [18].

Consider a generic nonlinear system

$$\dot{x} = f(x) + G(x)u, \qquad z = h(x), \tag{31}$$

where x is the system state, u is the input, and z is the output to which we wish to assign a desired behavior (e.g., track a given trajectory). Assume the system is square, i.e., the number of inputs equals the number of outputs.

The input-output linearization problem via static feedback consists in looking for a control law of the form

$$u = a(x) + B(x)r, \tag{32}$$

with $B(x)$ nonsingular and r an external auxiliary input of the same dimension as u, in such a way that the input-output response of the closed-loop system (i.e., between the new inputs r and the outputs z) is linear. In the multi-input multi-output case, the solution to this problem automatically yields input-output decoupling, namely, each component of the output z will depend only on a single component of the input r.

In general, a nonlinear *internal dynamics* which does not affect the input-output behavior may be left in the closed-loop system. This internal dynamics reduces to the so-called *clamped dynamics* when the output z is constrained to follow a desired trajectory $z_d(t)$. In the absence of internal dynamics, full-state linearization is achieved. Conversely, when only input-output linearization is obtained, the boundedness/stability of the internal dynamics should be analyzed in order to guarantee a feasible output tracking.

If static feedback does not allow to solve the problem, one can try to obtain the same results by means of a dynamic feedback compensator of the form

$$\begin{aligned} u &= a(x, \xi) + B(x, \xi) r \\ \dot{\xi} &= c(x, \xi) + D(x, \xi) r, \end{aligned} \tag{33}$$

where ξ is the compensator state of appropriate dimension. Again, the closed-loop system may or may not contain internal dynamics.

In its simplest form, which is suitable for the current application, the linearization algorithm proceeds by differentiating all system outputs until some of the inputs appear explicitly. At this point, one tries to invert the differential map in order to solve for the inputs. If the Jacobian of this map—referred to as the *decoupling matrix* of the system—is nonsingular, this procedure gives a static feedback law of the form (32) that solves the input-output linearization and decoupling problem.

If the decoupling matrix is singular, making it impossible to solve for all the inputs at the same time, one proceeds by adding integrators on a subset of the input channels. This operation, called *dynamic extension*, converts a system input into a state of a dynamic compensator, which is driven in turn by a new input. Differentiation of the outputs continues then until either it is possible to solve for the new inputs or the dynamic extension process has to be repeated. At the end, the number of added integrators will give the dimension of the state ξ of the nonlinear dynamic controller (33). The algorithm will terminate after a finite number of iterations if the system is *invertible* from the chosen outputs.

In any case, if the sum of the relative degrees (the order of differentiation of the outputs) equals the dimension of the (original or extended) state space, there is no internal dynamics and the same (static or dynamic, respectively) control law yields full-state linearization. In the following, we present both a static and a dynamic feedback controller for trajectory tracking.

3.3.1 Input-output linearization via static feedback

For the car-like robot model (5), the natural output choice for the trajectory tracking task is

$$z = \begin{bmatrix} x \\ y \end{bmatrix}.$$

The linearization algorithm begins by computing

$$\dot{z} = \begin{bmatrix} \cos\theta & 0 \\ \sin\theta & 0 \end{bmatrix} v = A(\theta) v. \tag{34}$$

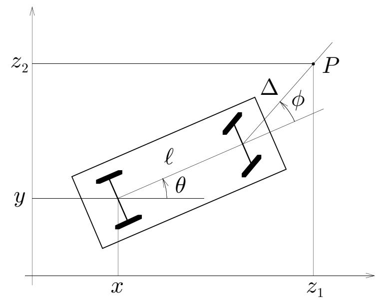

Figure 8: Alternative output definition for a car-like robot

At least one input appears in both components of $\dot{z}$, so that $A(\theta)$ is the actual decoupling matrix of the system. Since this matrix is singular, static feedback fails to solve the input-output linearization and decoupling problem.

A possible way to circumvent this problem is to redefine the system output as

$$z = \begin{bmatrix} x + \ell\cos\theta + \Delta\cos(\theta+\phi) \\ y + \ell\sin\theta + \Delta\sin(\theta+\phi) \end{bmatrix}, \tag{35}$$

with $\Delta \neq 0$. This choice corresponds to selecting the representative point of the robot as P in Fig. 8, in place of the midpoint of the rear axle.

Differentiation of this new output gives

$$\dot{z} = \begin{bmatrix} \cos\theta - \tan\phi(\sin\theta + \Delta\sin(\theta+\phi)/\ell) & -\Delta\sin(\theta+\phi) \\ \sin\theta + \tan\phi(\cos\theta + \Delta\cos(\theta+\phi)/\ell) & \Delta\cos(\theta+\phi) \end{bmatrix} v = A(\theta,\phi)v.$$

Since $\det A(\theta,\phi) = \Delta/\cos\phi \neq 0$, we can set $\dot{z} = r$ (an auxiliary input value) and solve for the inputs v as

$$v = A^{-1}(\theta,\phi)r.$$

In the globally defined transformed coordinates (z_1, z_2, θ, ϕ), the closed-loop system becomes

$$\begin{aligned} \dot{z}_1 &= r_1 \\ \dot{z}_2 &= r_2 \\ \dot{\theta} &= \sin\phi\,[\cos(\theta+\phi)r_1 + \sin(\theta+\phi)r_2]\,/\ell \\ \dot{\phi} &= -[\cos(\theta+\phi)\sin\phi/\ell + \sin(\theta+\phi)/\Delta]\,r_1 - [\sin(\theta+\phi)\sin\phi/\ell - \cos(\theta+\phi)/\Delta]\,r_2, \end{aligned} \tag{36}$$

which is input-output linear and decoupled (one integrator on each channel). We note that there exists a two-dimensional internal dynamics expressed by the differential equations for θ and ϕ.

In order to solve the trajectory tracking problem, we choose then

$$r_i = \dot{z}_{di} + k_{pi}(z_{di} - z_i), \qquad k_{pi} > 0, \qquad i = 1, 2, \tag{37}$$

obtaining exponential convergence of the output tracking error to zero, for any initial condition $(z_1(t_0), z_2(t_0), \theta(t_0), \phi(t_0))$. A series of remarks is now in order.

- While the two output variables converge to their reference trajectory with arbitrary exponential rate (depending on the choice of the k_{pi}'s in eq. (37)), the behavior of the variables θ and ϕ cannot be specified at will because it follows from the last two equations of (36).

- A complete analysis would require the study of the stability of the time-varying closed-loop system (36), with r given by eq. (37). In practice, one is interested in the boundedness of θ and ϕ along the nominal output trajectory. This study may not be trivial for higher-dimensional wheeled mobile robots, where the internal dynamics has dimension $n - 2$.

- Having redefined the system outputs as in eq. (35), one has two options for generating the reference output trajectory. The simplest choice is to directly plan a cartesian motion to be executed by the point P. On the other hand, if the planner generates a desired motion $x_d(t), y_d(t)$ for the rear axle midpoint (with associated $v_{d1}(t), v_{d2}(t)$ computed from eqs. (21) and (24)), this must be converted into a reference motion for P by forward integration of the car-like equations, with $v = v_d(t)$ and use of the output equation (35). In both cases, there is no smoothness requirement for $z_d(t)$ which may contain also discontinuities in the path tangent.

- The output choice (35) is not the only one leading to input-output linearization and decoupling by static feedback. As a matter of fact, the first two variables of the chained-form transformation (8) are another example of linearizing outputs, with static feedback given by (9).

3.3.2 Full-state linearization via dynamic feedback

In order to design a tracking controller directly for the cartesian outputs (x, y) of the car-like robot, dynamic extension is required in order to overcome the singularity of the decoupling matrix in eq. (34). Although the linearization procedure can be continued using the original kinematic description (5), we will apply it here to the chained-form representation (10) as a first step toward the extension to higher-dimensional systems.

In accordance with the task definition, choose the two system outputs as

$$z = \begin{bmatrix} x_1 \\ x_4 \end{bmatrix},$$

namely the x and y coordinates of the robot. Differentiating z with respect to time gives

$$\dot{z} = \begin{bmatrix} \dot{x}_1 \\ \dot{x}_4 \end{bmatrix} = \begin{bmatrix} 1 & 0 \\ x_3 & 0 \end{bmatrix} u,$$

where the input u_2 does not appear, so that the decoupling matrix is singular. In order to proceed with the differentiation, an integrator (with state denoted by ξ_1) is added on the first input

$$u_1 = \xi_1, \qquad \dot{\xi}_1 = u_1', \tag{38}$$

with u_1' a new auxiliary input. Using eq. (38), we can rewrite the first derivative of the output as

$$\dot{z} = \begin{bmatrix} \xi_1 \\ \xi_1 x_3 \end{bmatrix},$$

which is independent from the inputs u_1' and u_2 of the extended system. In this way, differentiation of the original input signal at the next step of the procedure is avoided. We have

$$\ddot{z} = \begin{bmatrix} \dot{\xi}_1 \\ \dot{x}_3\xi_1 + x_3\dot{\xi}_1 \end{bmatrix} = \begin{bmatrix} 0 \\ x_2\xi_1^2 \end{bmatrix} + \begin{bmatrix} 1 & 0 \\ x_3 & 0 \end{bmatrix} \begin{bmatrix} u_1' \\ u_2 \end{bmatrix}.$$

As u_2 does not appear yet, we add another integrator (with state denoted by ξ_2) on the input u_1'

$$u_1' = \xi_2, \qquad \dot{\xi}_2 = u_1'', \tag{39}$$

obtaining

$$\ddot{z} = \begin{bmatrix} \xi_2 \\ x_2\xi_1^2 + x_3\xi_2 \end{bmatrix}.$$

Finally, the last differentiation gives

$$\dddot{z} = \begin{bmatrix} 0 \\ 3x_2\xi_1\xi_2 \end{bmatrix} + \begin{bmatrix} 1 & 0 \\ x_3 & \xi_1^2 \end{bmatrix} \begin{bmatrix} u_1'' \\ u_2 \end{bmatrix}. \tag{40}$$

The matrix weighting the inputs is nonsingular provided that $\xi_1 \neq 0$. Under such assumption—on which we will come back later—we set $\dddot{z} = r$ (an auxiliary input value) and solve eq. (40) for

$$\begin{bmatrix} u_1'' \\ u_2 \end{bmatrix} = \begin{bmatrix} r_1 \\ (r_2 - x_3r_1 - 3x_2\xi_1\xi_2)/\xi_1^2 \end{bmatrix}. \tag{41}$$

Putting together the dynamic extensions (38) and (39) with eq. (41), the resulting nonlinear dynamic feedback controller

$$\begin{aligned} u_1 &= \xi_1 \\ u_2 &= (r_2 - x_3 r_1 - 3x_2\xi_1\xi_2)/\xi_1^2 \\ \dot{\xi}_1 &= \xi_2 \\ \dot{\xi}_2 &= r_1 \end{aligned} \tag{42}$$

transforms the original system into two decoupled chains of three input-output integrators

$$\begin{aligned} \dddot{z}_1 &= r_1 \\ \dddot{z}_2 &= r_2. \end{aligned}$$

The original system in chained form had four states, whereas the dynamic controller has two additional states. All these six states are found in the above input-output description, and hence there is no internal dynamics left. Thus, full-state linearization has been obtained.

On the linear and decoupled system, it is easy to complete the control design with a globally stabilizing feedback for the desired trajectory (independently on each integrator chain). To this end, let

$$r_i = \dddot{z}_{di} + k_{ai}(\ddot{z}_{di} - \ddot{z}_i) + k_{vi}(\dot{z}_{di} - \dot{z}_i) + k_{pi}(z_{di} - z_i), \qquad i = 1, 2, \tag{43}$$

where the feedback gains are such that the polynomials

$$\lambda^3 + k_{ai}\lambda^2 + k_{vi}\lambda + k_{pi}, \qquad i = 1, 2,$$

are Hurwitz, and z, $\dot{z}$, $\ddot{z}$ are computed from the intermediate steps of the dynamic extension algorithm as

$$\begin{aligned} z &= \begin{bmatrix} x_1 \\ x_4 \end{bmatrix} \\ \dot{z} &= \begin{bmatrix} \xi_1 \\ x_3\xi_1 \end{bmatrix} \\ \ddot{z} &= \begin{bmatrix} \xi_2 \\ x_2\xi_1^2 + x_3\xi_2 \end{bmatrix}. \end{aligned} \tag{44}$$

In order to initialize the chained-form system and the associated dynamic controller for exact reproduction of the desired output trajectory, we can set $z = z_d(t)$

and solve eqs. (44) at time $t = t_0$:

$$\begin{aligned}
x_1(t_0) &= z_{d1}(t_0) \quad (= x_d(t_0)) \\
x_2(t_0) &= \left[\dot{z}_{d1}(t_0)\ddot{z}_{d2}(t_0) - \ddot{z}_{d1}(t_0)\dot{z}_{d2}(t_0)\right] / \dot{z}_{d1}^3(t_0) \\
x_3(t_0) &= \dot{z}_{d2}(t_0)/\dot{z}_{d1}(t_0) \\
x_4(t_0) &= z_{d2}(t_0) \quad (= y_d(t_0)) \\
\xi_1(t_0) &= \dot{z}_{d1}(t_0) \\
\xi_2(t_0) &= \ddot{z}_{d1}(t_0).
\end{aligned}$$

Any other initialization of the robot and/or the dynamic controller will produce a transient state error that converges exponentially to zero, with the rate specified by the chosen gains in eq. (43).

As mentioned in Sect. 3.1, only trajectories $z_d(t) = (x_d(t), y_d(t))$ with continuous second time derivatives are exactly reproducible. In the presence of lesser smoothness, the car-like robot will deviate from the desired trajectory. Nonetheless, after the occurrence of isolated discontinuities, the feedback controller (42–43) will be able to drive the vehicle back to the remaining part of the smooth trajectory at an exponential rate.

The above approach can be easily extended to the general case of the $(2, n)$ chained form (7). In fact, such representation can be fully transformed via dynamic feedback into decoupled strings of input-output integrators by defining the system output as (x_1, x_n). This result is summarized in the following proposition.

Proposition 1 *Consider the $(2, n)$ chained-form system (7) and define its output as*

$$z = \begin{bmatrix} x_1 \\ x_n \end{bmatrix}. \tag{45}$$

By using a nonlinear dynamic feedback controller of dimension $n - 2$, the system can be fully transformed into a linear one consisting of two decoupled chains of $n-1$ integrators, provided that $u_1 \neq 0$.

Proof We will provide a constructive solution. Let the dynamic extension be composed of $n - 2$ integrators added on input u_1

$$u_1^{(n-2)} = \bar{u}_1, \tag{46}$$

with the input u_2 unchanged. Denote the states of these integrators by $\xi_1, \ldots, \xi_{n-2}$, so that a state-space representation of eq. (46) is

$$
\begin{aligned}
u_1 &= \xi_1 \\
\dot{\xi}_1 &= \xi_2 \\
\dot{\xi}_2 &= \xi_3 \\
&\vdots \\
\dot{\xi}_{n-2} &= \bar{u}_1.
\end{aligned} \tag{47}
$$

The extended system consisting of eqs. (7) and (47) is

$$
\begin{aligned}
\dot{x}_1 &= \xi_1 \\
\dot{x}_2 &= u_2 \\
\dot{x}_3 &= x_2\xi_1 \\
\dot{x}_4 &= x_3\xi_1 \\
&\vdots \\
\dot{x}_{n-1} &= x_{n-2}\xi_1 \\
\dot{x}_n &= x_{n-1}\xi_1 \\
\dot{\xi}_1 &= \xi_2 \\
\dot{\xi}_2 &= \xi_3 \\
&\vdots \\
\dot{\xi}_{n-3} &= \xi_{n-2} \\
\dot{\xi}_{n-2} &= \bar{u}_1.
\end{aligned} \tag{48}
$$

By applying the linearization algorithm, we have for the first few derivatives of the output (45):

$$
\begin{aligned}
\dot{z} &= \begin{bmatrix} \xi_1 \\ x_{n-1}\xi_1 \end{bmatrix} \\
\ddot{z} &= \begin{bmatrix} \xi_2 \\ x_{n-2}\xi_1^2 + x_{n-1}\xi_2 \end{bmatrix} \\
\dddot{z} &= \begin{bmatrix} \xi_3 \\ x_{n-3}\xi_1^3 + x_{n-1}\xi_3 + 3\xi_1\xi_2 x_{n-2} \end{bmatrix} \\
z^{(4)} &= \begin{bmatrix} \xi_4 \\ x_{n-4}\xi_1^4 + x_{n-1}\xi_4 + (6\xi_1^2\xi_2 x_{n-3} + 4\xi_1\xi_3 x_{n-2} + 3\xi_2^2 x_{n-2}) \end{bmatrix}, \\
&\vdots
\end{aligned}
$$

so that the structure of the $(n-2)$-th derivative is

$$z^{(n-2)} = \left[\begin{array}{c} \xi_{n-2} \\ x_2 \xi_1^{n-2} + x_{n-1}\xi_{n-2} + f(\xi_1, \xi_2, \dots, \xi_{n-3}, x_3, x_4, \dots, x_{n-2}) \end{array} \right],$$

where f is a polynomial function of its arguments. The expressions of the output (45) together with its derivatives up to the $(n-2)$-th order induce a diffeomorphism between $(x_1, \dots, x_n, \xi_1, \dots, \xi_{n-2})$ and $(z, \dot{z}, \dots, z^{(n-2)})$, which is globally defined except for the manifold $\xi_1 = 0$.

We obtain finally

$$z^{(n-1)} = \left[\begin{array}{c} 0 \\ g(\xi_1, \xi_2, \dots, \xi_{n-2}, x_2, x_3, \dots, x_{n-2}) \end{array} \right] + \left[\begin{array}{cc} 1 & 0 \\ x_{n-1} & \xi_1^{n-2} \end{array} \right] \left[\begin{array}{c} \bar{u}_1 \\ u_2 \end{array} \right], \qquad (49)$$

where g is a polynomial function of its arguments. The decoupling matrix of the extended system is nonsingular provided that $\xi_1 \neq 0$ or, equivalently, that $u_1 \neq 0$. Under this assumption, we can set $z^{(n-1)} = r$ and solve eq. (49) for $(\bar{u}_1, u_2)$. Reorganizing with eq. (47), we conclude that the following nonlinear dynamic controller of dimension $n-2$

$$\begin{array}{rcl} u_1 & = & \xi_1 \\ u_2 & = & [r_2 - x_{n-1} r_1 - g(\xi_1, \xi_2, \dots, \xi_{n-2}, x_2, x_3, \dots, x_{n-2})]/\xi_1^{n-2} \\ \dot{\xi}_1 & = & \xi_2 \\ & \vdots & \\ \dot{\xi}_{n-3} & = & \xi_{n-2} \\ \dot{\xi}_{n-2} & = & r_1 \end{array} \qquad (50)$$

transforms the original chained-form system (7) with output (45) into the input-output linear and decoupled system

$$z^{(n-1)} = \left[\begin{array}{c} x_1^{(n-1)} \\ x_n^{(n-1)} \end{array} \right] = \left[\begin{array}{c} r_1 \\ r_2 \end{array} \right] = r.$$

Since the number of the input-output integrators $(2(n-1))$ equals the number of states of the extended system $(n + (n-2))$, there is no internal dynamics in the closed-loop system and thus we have obtained full-state linearization and input-output decoupling. ∎

The above result indicates that dynamic feedback linearization offers a viable control design tool for trajectory tracking, even for higher-dimensional kinematic models of wheeled mobile robots (e.g., the N-trailer system). The same dynamic extension technique can be directly applied to the original kinematic equations of the wheeled mobile robot, without resorting to the chained-form transformation. In particular, for the car-like robot (5), similar computations show that the dynamic controller takes the form:

$$\begin{aligned} v_1 &= \xi_1 \\ v_2 &= -3\xi_2 \cos^2\phi \tan\phi/\xi_1 - \ell r_1 \cos^2\phi \sin\theta/\xi_1^2 + \ell r_2 \cos^2\phi \cos\theta/\xi_1^2 \\ \dot{\xi}_1 &= \xi_2 \\ \dot{\xi}_2 &= \xi_1^3 \tan^2\phi/\ell^2 + r_1 \cos\theta + r_2 \sin\theta. \end{aligned} \tag{51}$$

The external inputs r_1 and r_2 are chosen as in (43), with the values of z, $\dot{z}$ and $\ddot{z}$ given by

$$\begin{aligned} z &= \begin{bmatrix} x \\ y \end{bmatrix} \\ \dot{z} &= \begin{bmatrix} \xi_1 \cos\theta \\ \xi_1 \sin\theta \end{bmatrix} \\ \ddot{z} &= \begin{bmatrix} -\xi_1^2 \tan\phi \sin\theta/\ell + \xi_2 \cos\theta \\ \xi_1^2 \tan\phi \cos\theta/\ell + \xi_2 \sin\theta \end{bmatrix}. \end{aligned} \tag{52}$$

The derivation of the initial conditions on (x, y, θ, ϕ) and (ξ_1, ξ_2) allowing for exact reproduction of a smooth trajectory is straightforward using eqs. (52).

The main limitation of the dynamic feedback linearization approach is the requirement that the compensator state variable ξ_1 (which corresponds to v_1 if linearization is performed on the original car-like equations, or to u_1 if it is performed on its chained-form representation) should never be zero. In fact, in this case the second control input (i.e., v_2 in eq. (51) and u_2 in eq. (42) or, more in general, in eq. (50)) could diverge. It has been shown that the occurrence of this singularity in the dynamic extension process is structural for nonholonomic systems [14]. Therefore, this approach as such is feasible only for trajectory tracking.

In addition, note the following facts with specific reference to the controller (51–52) for the car-like robot.

- If the desired trajectory is smooth and persistent, the nominal control input v_{d1} does not decay to zero. As the robot is guaranteed to converge exponentially to the desired trajectory, also the actual command v_1 will eventually be bounded away from zero. On the other hand, exact reproduction of trajectories with linear velocity vanishing to zero (e.g., trajectories with cusps, where the robot should stop and reverse the direction of motion) is not allowed with this control scheme.

- Even for smooth persistent trajectories, problems may arise if the command v_1 crosses zero during an initial transient. However, this situation can be avoided by suitably choosing the initialization of the dynamic controller (i.e., the states ξ_1 and ξ_2), which is in practice an additional degree of freedom in the design. As a matter of fact, a simple way to keep the actual commands bounded is to reset the state ξ_1 whenever its value falls below a given threshold. Note that this would result in an input command v that is discontinuous with respect to time.

The problem of tracking a trajectory starting (or ending) with zero linear velocity using the above approach can be solved by separating geometric from timing information in the control law, along the same lines indicated in Sect. 3.1. Suppose that a smooth path of finite length L has to be tracked starting and ending with zero velocity, and let σ be the path parameter. The timing law $\sigma(t)$ can be any increasing function such that

$$\sigma(0) = 0, \quad \sigma(T) = L, \quad \dot{\sigma}(0) = \dot{\sigma}(T) = 0,$$

where T is the final time at which the motion ends. The car-like equations can be rewritten in the path parameter domain as

$$\begin{aligned} x' &= \cos\theta\, w_1 \\ y' &= \sin\theta\, w_1 \\ \theta' &= \tan\phi\, w_1/\ell \\ \phi' &= w_2, \end{aligned} \tag{53}$$

with the actual velocity commands v_i related to the new inputs w_i by

$$v_i(t) = w_i(\sigma(t))\dot{\sigma}(t), \qquad i = 1, 2.$$

For system (53), one can design a dynamic feedback achieving full-state linearization as before. In this case, tracking errors will converge exponentially to zero in the σ-domain (instead of the t-domain). Moreover, the control law is always well-defined since it is possible to show that in the denominator of w_2 only the linear pseudovelocity w_1 appears, a geometric quantity which is always nonzero being related to the path tangent.

3.3.3 Simulation results

In order to compare the performance of linear and nonlinear control design, the nonlinear dynamic controller (42-43) computed for the chained-form representation has been used to track the same sinusoidal trajectory (27) of Sect. 3.2. The initial condition at $t_0 = 0$ of the car-like robot (of length $\ell = 1$ m) is the same as before (off the trajectory)

$$x_1(0) = -2, \quad x_2(0) = 0, \quad x_3(0) = A\,\omega, \quad x_4(0) = -1,$$

with the initial state of the dynamic compensator set at

$$\xi_1(0) = 1, \quad \xi_2(0) = 0.$$

As for the stabilizing part of the controller, we have chosen the same gains for both input-output channels, with three coincident closed-loop eigenvalues located at -5 ($k_{ai} = 15$, $k_{vi} = 75$, $k_{pi} = 125$, $i = 1, 2$).

The results are shown in Figs. 9–11, again in terms of errors on the original states x, y, θ and ϕ, and of the actual control inputs v_1, v_2 for the car-like robot. A comparison with the analogous plots in Figs. 5–7 shows that the peaks of the transient errors are approximately halved in this particular case. Also, the control effort on the linear velocity v_1 in Fig. 11 does not reach the large initial value of Fig. 7, while the control input v_2 has a lower average value. After achieving convergence, the input commands of the nonlinear dynamic controller are identical to those of the linear one, for they both reduce to the nominal feedforward needed to execute the desired trajectory. Moreover, as a result of the imposed linear dynamics of the feedback controlled system, the transient behavior of the errors is globally exponentially converging to zero, i.e., for any initial conditions of the car-like robot and of the dynamic compensator.

We have also simulated the dynamic feedback controller (51–52) designed directly on the car-like model. Results for a circular and an eight-shaped trajectory are reported in Figs. 12–19, assuming a length $\ell = 0.1$ m for the car. Note that the small peak of the x error in Fig. 13 is only due to an initial mismatch of the robot state with respect to the value specified by the higher-order derivatives of $x_d(t)$ (in particular, of $\dot{x}_d(0)$). In fact, in view of the decoupling property induced by the controller, the value of the initial error along each cartesian direction does not affect the error behavior and the control action in the other direction.

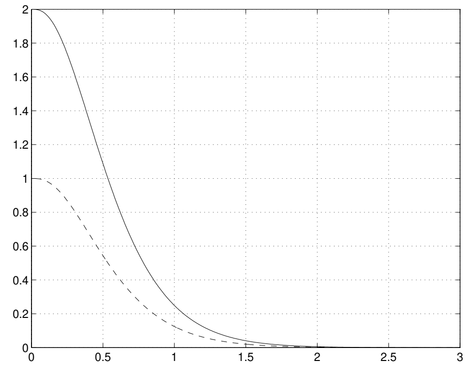

Figure 9: Tracking a sinusoid with dynamic feedback linearization: x (—), y (−−) errors (m) vs. time (sec)

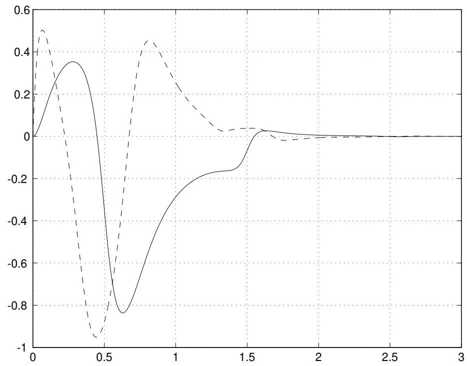

Figure 10: Tracking a sinusoid with dynamic feedback linearization: θ (—), ϕ (−−) errors (rad) vs. time (sec)

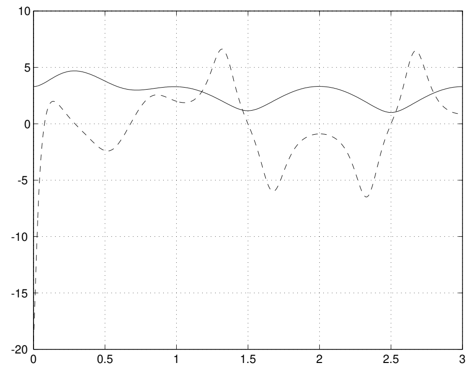

Figure 11: Tracking a sinusoid with dynamic feedback linearization: v_1 (—) (m/sec), v_2 (−−) (rad/sec) vs. time (sec)

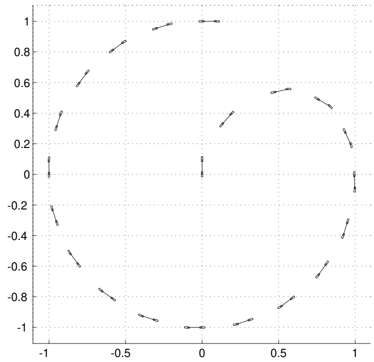

Figure 12: Tracking a circle with dynamic feedback linearization: stroboscopic view of the cartesian motion

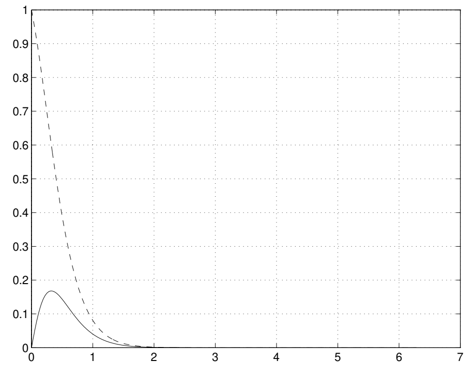

Figure 13: Tracking a circle with dynamic feedback linearization: x (—), y (−−) errors (m) vs. time (sec)

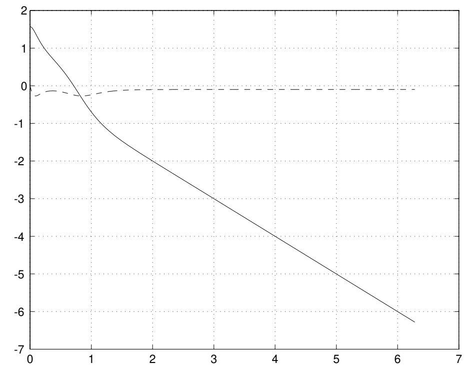

Figure 14: Tracking a circle with dynamic feedback linearization: θ (—), ϕ (−−) (rad) vs. time (sec)

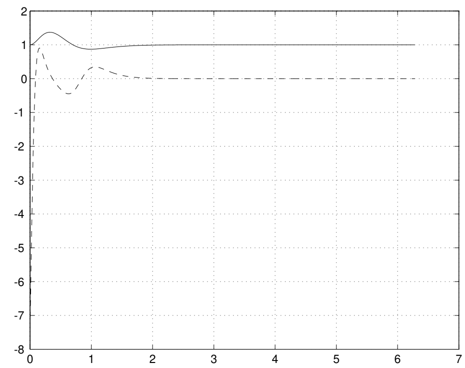

Figure 15: Tracking a circle with dynamic feedback linearization: v_1 (—) (m/sec), v_2 ($--$) (rad/sec) vs. time (sec)

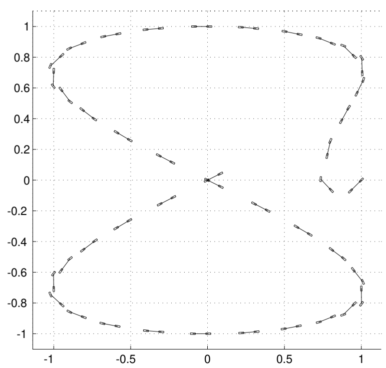

Figure 16: Tracking an eight figure with dynamic feedback linearization: stroboscopic view of the cartesian motion

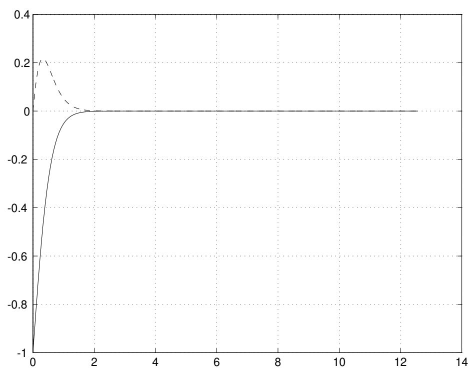

Figure 17: Tracking an eight figure with dynamic feedback linearization: x (—), y ($--$) errors (m) vs. time (sec)

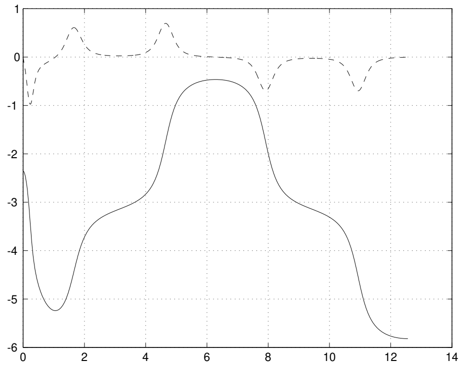

Figure 18: Tracking an eight figure with a dynamic feedback linearization: θ (—), ϕ ($--$) (rad) vs. time (sec)

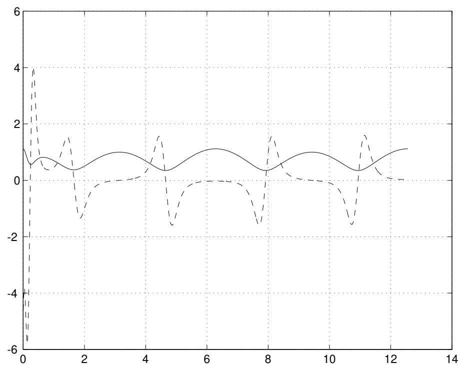

Figure 19: Tracking an eight figure with a dynamic feedback linearization: v_1 (—) (m/sec), v_2 ($--$) (rad/sec) vs. time (sec)

4 Path Following and Point Stabilization

In this section, we address the problem of driving the car-like robot to a desired, fixed configuration by using only the current error information, without the need of planning a trajectory joining the initial point to the final destination. In doing this, a control solution for the path following task is obtained as an intermediate step.

As shown in Sect. 2, for nonholonomic mobile robots the point stabilization problem is considerably more difficult than trajectory tracking and path following. In particular, smooth pure state feedback does not solve the problem. Recently, the idea of including an exogenous time-varying signal in the controller has proven to be successful for achieving asymptotic stability [38]. Roughly speaking, the underlying logic is that such a signal allows all components of the configuration error to be reflected on the control inputs, so that the error itself can be asymptotically reduced to zero.

Some physical insight on the role of time-varying feedback can be gained by thinking about a parallel parking maneuver of a real car. We can reasonably assume that a human driver controls the vehicle through a front wheel steering command and a linear velocity command. In order to bring to zero the error in the lateral direction—along which the car cannot move directly—experience indicates that an approximately periodic forward/backward motion should be imposed to the car. This motion is somewhat independent from the lateral position error with respect to the goal and is used only to sustain the generation of a net side motion through the combined action of the steering command, which is instead a function of the position error.

Although natural, this strategy is hard to generalize to more complex vehicle kinematics, whose maneuverability is less intuitive. For this reason, we have chosen to present here two methods of wide applicability that are designed on the chained-form representation of the system. In order to emphasize the generality of the controller design, the case of an n-dimensional system is considered. We give, however, some details for the case $n = 4$.

Both the presented feedback laws are time-varying, but they differ in their dependence from the current state as well as in some methodological aspects. The first control is either smooth or at least continuous with respect to the robot state. The second is nonsmooth, in the sense that the state is measured and fed back only at discrete instants of time. Nevertheless, discarding this time-discretization aspect, it is also basically continuous with respect to the state at the desired configuration, contrary to other time-invariant discontinuous feedback laws (see Sect. 6). Both controllers provide inputs that are continuous with respect to time and are globally defined on the chained-form representation.

Throughout this section, it will be assumed without loss of generality that the desired configuration coincides with the origin of the state space.

4.1 Control via smooth time-varying feedback

The smooth feedback stabilization method presented here was proposed in [44]. It exploits the internal structure of chained systems in order to decompose the solution approach in two design phases. In the first phase, it is assumed that one control input is given and satisfies some general requirements. The other control is then designed for achieving stabilization of an $(n-1)$-dimensional subvector of the system state. At this stage, a solution to the path following problem has already been obtained.

In the second phase, the design is completed by specifying the first control so as to guarantee convergence of the remaining variable while preserving the overall closed-loop stability.

As a preliminary step, reorder for convenience the variables of the chained form by letting

$$\mathcal{X} = (\chi_1, \chi_2, \ldots, \chi_{n-1}, \chi_n) = (x_1, x_n, \ldots, x_3, x_2).$$

As a consequence, the chained form system (7) becomes

$$\begin{aligned} \dot{\chi}_1 &= u_1 \\ \dot{\chi}_2 &= \chi_3 u_1 \\ \dot{\chi}_3 &= \chi_4 u_1 \\ &\vdots \\ \dot{\chi}_{n-1} &= \chi_n u_1 \\ \dot{\chi}_n &= u_2, \end{aligned} \tag{54}$$

or equivalently

$$\dot{\mathcal{X}} = h_1(\mathcal{X}) u_1 + h_2 u_2, \qquad h_1(\mathcal{X}) = \begin{bmatrix} 1 \\ \chi_3 \\ \chi_4 \\ \vdots \\ \chi_n \\ 0 \end{bmatrix}, \quad h_2 = \begin{bmatrix} 0 \\ 0 \\ 0 \\ \vdots \\ 0 \\ 1 \end{bmatrix}. \tag{55}$$

For the car-like robot, the above reordering is simply an exchange between the second and fourth coordinates. Therefore, the cartesian position of the rear wheel is (χ_1, χ_2). Analogously, for an N-trailer robot, χ_1 and χ_2 represent the cartesian coordinates of the midpoint of the last trailer axle.

Let $\mathcal{X} = (\chi_1, \mathcal{X}_2)$, with $\mathcal{X}_2 = (\chi_2, \chi_3, \ldots, \chi_n)$. In the following, we shall first pursue the stabilization of $\mathcal{X}_2$ to zero, and then the complete stabilization of $\mathcal{X}$ to the origin.

4.1.1 Path following via input scaling

When u_1 is assigned as a function of time, the chained system (55) can be written as

$$
\begin{aligned}
\dot{\tilde{\chi}}_1 &= 0 \\
\dot{\mathcal{X}}_2 &= \begin{bmatrix} 0 & u_1(t) & 0 & \cdots & \cdots & 0 \\ 0 & 0 & u_1(t) & 0 & \cdots & 0 \\ \vdots & & & & & \vdots \\ 0 & \cdots & \cdots & \cdots & u_1(t) & 0 \\ 0 & \cdots & \cdots & \cdots & 0 & u_1(t) \\ 0 & 0 & \cdots & \cdots & \cdots & 0 \end{bmatrix} \mathcal{X}_2 + \begin{bmatrix} 0 \\ 0 \\ \vdots \\ 0 \\ 0 \\ 1 \end{bmatrix} u_2,
\end{aligned}
\tag{56}
$$

having set

$$\tilde{\chi}_1 = \chi_1 - \int_0^t u_1(\tau) d\tau.$$

The first equation in (56) clearly shows that, when the input u_1 is a priori assigned, the system is no more controllable. However, the structure of the differential equations for $\mathcal{X}_2$ is reminiscent of the controllable canonical form for linear systems. In particular, when u_1 is constant and nonzero, system (56) becomes time-invariant and its second part is clearly controllable. As a matter of fact, controllability holds whenever $u_1(t)$ is a piecewise-continuous, bounded, and strictly positive (or negative) function. Under these assumptions, x_1 varies monotonically with time and differentiation with respect to time can be replaced by differentiation with respect to χ_1, being

$$\frac{d}{dt} = \frac{d}{d\chi_1}\dot{\chi}_1 = \frac{d}{d\chi_1} u_1,$$

and thus

$$\operatorname{sign}(u_1)\frac{d}{d\chi_1} = \frac{1}{|u_1|} \cdot \frac{d}{dt}.$$

This change of variable is equivalent to an input scaling procedure (see Sect. 3.2). Then, the second part of the system may be rewritten as

$$
\begin{aligned}
\chi_2^{[1]} &= \operatorname{sign}(u_1)\chi_3 \\
\chi_3^{[1]} &= \operatorname{sign}(u_1)\chi_4 \\
&\vdots \\
\chi_{n-1}^{[1]} &= \operatorname{sign}(u_1)\chi_n \\
\chi_n^{[1]} &= \operatorname{sign}(u_1)u_2',
\end{aligned}
\tag{57}
$$

with the definitions

$$\chi_i^{[j]} = \operatorname{sign}(u_1)\frac{d^j \chi_i}{d\chi_1^j} \quad \text{and} \quad u_2' = \frac{u_2}{u_1}.$$

Equation (57) is a linear time-invariant system, an equivalent input-output representation of which is

$$\chi_2^{[n-1]} = \mathrm{sign}(u_1)^{n-1} u_2'.$$

Such system is controllable and admits an exponentially stable linear feedback in the form

$$u_2'(\mathcal{X}_2) = -\mathrm{sign}(u_1)^{n-1} \sum_{i=1}^{n-1} k_i \chi_2^{[i-1]}, \tag{58}$$

where the gains $k_i > 0$ are chosen so as to satisfy the Hurwitz stability criterion. Hence, the time-varying control

$$u_2(\mathcal{X}_2, t) = u_1(t) u_2'(\mathcal{X}_2) \tag{59}$$

globally asymptotically stabilizes the origin $\mathcal{X}_2 = 0$.

The above approach provides a solution to the path following problem. Consider in particular the case of a car-like robot. We have seen at the end of Sect. 2.3 that the system equations (14) in path coordinates can be transformed in chained form. By reordering the variables as in eq. (54), χ_1 represents the arc length s along the path, χ_2 is the distance d between the car and the path, while χ_3 and χ_4 are related to the car steering angle ϕ and to the relative orientation θ_p between the path and the car. Path following requires zeroing the χ_2, χ_3 and χ_4 variables (i.e., $\mathcal{X}_2 = 0$), independently from χ_1. Then, for any piecewise-continuous, bounded, and strictly positive (or negative) u_1, eq. (58) is particularized as

$$u_2'(\chi_2, \chi_3, \chi_4) = -\mathrm{sign}(u_1)[k_1\chi_2 + k_2 \,\mathrm{sign}(u_1)\chi_3 + k_3\chi_4].$$

Using eq. (59), the path following feedback control law is

$$u_2(\chi_2, \chi_3, \chi_4, t) = -k_1|u_1(t)|\chi_2 - k_2 u_1(t)\chi_3 - k_3|u_1(t)|\chi_4,$$

which can be compared with eq. (30) to appreciate the analogy. Such an approach was originally proposed in [42] for the path following of a unicycle. From the above developments, it is clear that it can be applied to any mobile robot which can be converted into chained form.

4.1.2 Skew-symmetric chained forms and Lyapunov control design

We show now, by introducing a modified chained form, that it is possible to stabilize globally the origin $\mathcal{X}_2 = 0$ under more general hypotheses, namely that $|u_1(t)|$, $|\dot{u}_1(t)|$ are bounded and $u_1(t)$ does not asymptotically tend to zero. An important difference with respect to the previous analysis is that $u_1(t)$ is allowed to pass through zero.

From there, it will be relatively simple to derive a class of smooth time-varying feedback laws which stabilize globally the origin $\mathcal{X} = 0$ of the complete system (point stabilization).

Consider the following change of coordinates

$$\begin{aligned} z_1 &= \chi_1 \\ z_2 &= \chi_2 \\ z_3 &= \chi_3 \\ z_{j+3} &= k_j z_{j+1} + L_{h_1} z_{j+2}, \qquad j = 1, \ldots, n-3, \end{aligned} \tag{60}$$

where k_j ($j = 1, \ldots, n-3$) is a real positive number and $L_{h_1} z_j = \frac{\partial z_j}{\partial \mathcal{X}} h_1(\mathcal{X})$ is the Lie derivative of z_j along the vector field h_1. One easily verifies that eq. (60) is a linear, invertible change of coordinates, since the associated Jacobian matrix is of full rank. In particular, $\mathcal{X} = 0$ and $\mathcal{X}_2 = 0$ are respectively equivalent to $Z = 0$ and $Z_2 = 0$, having set $Z = (z_1, Z_2)$, $Z_2 = (z_2, z_3, \ldots, z_n)$. Moreover, it is $L_{h_2} z_i = 0$ ($i = 1, \ldots, n-1$) and $L_{h_2} z_n = 1$.

Taking the time derivative of z_{j+3} and using eq. (55) gives

$$\dot{z}_{j+3} = \frac{\partial z_{j+3}}{\partial \mathcal{X}} \dot{\mathcal{X}} = (L_{h_1} z_{j+3}) u_1 + (L_{h_2} z_{j+3}) u_2,$$

and from eq. (60)

$$L_{h_1} z_{j+3} = -k_{j+1} z_{j+2} + z_{j+4}.$$

As a result, we obtain

$$\dot{z}_{j+3} = (-k_{j+1} z_{j+2} + z_{j+4}) u_1 \qquad j = 0, \ldots, n-4$$

and for the last differential equation

$$\dot{z}_n = L_{h_1} z_n u_1 + u_2.$$

The original chained system (54) has thus been converted into the following *skew-symmetric* chained form

$$\begin{aligned} \dot{z}_1 &= u_1 \\ \dot{z}_2 &= u_1 z_3 \\ \dot{z}_{j+3} &= -k_{j+1} u_1 z_{j+2} + u_1 z_{j+4}, \qquad j = 0, \ldots, n-4, \\ \dot{z}_n &= -k_{n-2} u_1 z_{n-1} + w_2, \end{aligned} \tag{61}$$

where it was convenient to define the new input signal

$$w_2 = (k_{n-2} z_{n-1} + L_{h_1} z_n) u_1 + u_2. \tag{62}$$

The skew-symmetric structure of the above form is clear when writing the system as follows

$$
\begin{aligned}
\dot{z}_1 &= u_1 \\
\dot{Z}_2 &= \mathrm{diag}\{1, k_1, k_1 k_2, \ldots, \prod_{j=1}^{n-2} k_j\} \cdot (S(u_1) Z_2 + b\, w_2)\,,
\end{aligned}
$$

where

$$
S(u_1) = \begin{bmatrix}
0 & u_1 & & & & \\
-u_1 & 0 & \frac{u_1}{k_1} & & & \\
 & -\frac{u_1}{k_1} & 0 & \frac{u_1}{k_1 k_2} & & \\
 & & -\frac{u_1}{k_1 k_2} & 0 & & \\
 & & & \cdots & & \\
 & & & & 0 & \frac{u_1}{\prod_{j=1}^{n-3} k_j} \\
 & & & & -\frac{u_1}{\prod_{j=1}^{n-3} k_j} & 0
\end{bmatrix}, \qquad
b = \begin{bmatrix} 0 \\ 0 \\ \vdots \\ \vdots \\ 0 \\ \frac{1}{\prod_{j=1}^{n-2} k_j} \end{bmatrix}.
$$

The interest of the skew-symmetric form is that it is naturally suited for a Lyapunov-like analysis, as illustrated by the following result.

Proposition 2 *Assume that $|u_1(t)|$ and $|\dot{u}_1(t)|$ are bounded, and let*

$$
w_2 = -k_{w_2}(u_1) z_n, \tag{63}
$$

where $k_{w_2}(\cdot)$ is a continuous application strictly positive on $I\!R - \{0\}$. If this control law is applied to system (61), the positive function

$$
V(Z_2) = \frac{1}{2}\left(z_2^2 + \frac{1}{k_1} z_3^2 + \frac{1}{k_1 k_2} z_4^2 + \cdots + \frac{1}{\prod_{j=1}^{n-2} k_j} z_n^2 \right)
$$

is nonincreasing along the closed-loop system solutions and asymptotically converges to a limit value $V_{\lim}$ which depends on the initial conditions. Moreover, if $u_1(t)$ does not asymptotically tend to zero, it is $V_{\lim} = 0$ and the origin $Z_2 = 0$ is globally asymptotically stable.

Proof Computing the time derivative of V, using the last $n-1$ equations in (61) and the skew-symmetry of the system matrix, one obtains:

$$
\dot{V} = \frac{\partial V}{\partial Z_2} \dot{Z}_2 = Z_2^T \left[S(u_1) Z_2 + b\, w_2 \right] = \frac{1}{\prod_{j=1}^{n-2} k_j} z_n w_2 .
$$

Hence, using the control law (63)

$$\dot{V} = -\frac{k_{w_2}(u_1)}{\prod_{j=1}^{n-2} k_j} z_n^2 \leq 0, \tag{64}$$

which shows that the Lyapunov-like function V is nonincreasing. This in turn implies that $\|Z_2\|$ is bounded uniformly with respect to the initial conditions. Existence and uniqueness of the system solutions also follows.

Since V is nonincreasing and bounded below, it converges to a non-negative limit value $V_{\lim}$. Also, $k_{w_2}(u_1)$ is uniformly continuous as a function of time because $k_{w_2}(\cdot)$ is continuous and $|u_1(t)|$, $|\dot{u}_1(t)|$ are bounded. Hence, the right-hand side of eq. (64) is uniformly continuous along any system solution and, by application of Barbalat's lemma [20], $\dot{V}$ tends to zero. Therefore, $k_{w_2}(u_1)z_n$ tends to zero. This in turn implies, using the properties of the function $k_{w_2}(\cdot)$ and the boundedness of $|u_1(t)|$ and $|z_n(t)|$, that $u_1(t)z_n(t)$ tends to zero.

We can now proceed in a recursive fashion, exploiting the structure of eq. (61). Taking the time derivative of $u_1^2 z_n$, and using the convergence of $u_1 z_n$ to zero, one gets

$$\frac{d}{dt}(u_1^2 z_n) = -k_{n-2} u_1^3 z_{n-1} + o(t), \qquad \text{with } \lim_{t \to +\infty} o(t) = 0. \tag{65}$$

The function $u_1^3 z_{n-1}$ is uniformly continuous along any system solution because its time derivative is bounded. Therefore, in view of eq. (65) and since $u_1^2 z_n$ tends to zero, $d(u_1^2 z_n)/dt$ also tends to zero (by application of a slightly generalized version of Barbalat's lemma). Hence, both $u_1^3 z_{n-1}$ and $u_1 z_{n-1}$ tend to zero. Taking the time derivative of $u_1^2 z_j$ and repeating the above procedure, one concludes that $u_1 z_j$ tends to zero for $j = 2, \ldots, n$. Through the system equations, this in turn implies the convergence of $\dot{Z}_2$ to zero.

Summing up the squared values of $u_1 z_j$ for $j = 2, \ldots, n$, it is clear that also $u_1^2 V$ tends to zero, together with $u_1 V$. From the already established convergence of $V(t)$ to $V_{\lim}$, we have also that $u_1 V_{\lim}$ tends to zero, implying $V_{\lim} = 0$ if $u_1(t)$ does not asymptotically tend to zero. ∎

Once a signal $u_1(t)$ satisfying the hypotheses of Prop. 2 has been chosen, we must design a suitable function $k_{w_2}(u_1)$ and select the constants k_j ($j = 1, \ldots, n-2$) appearing in the definition (60) of the skew-symmetric coordinates z_i ($i = 4, \ldots, n$) and in the control signal (62). As it is often the case, tuning several control parameters may be rather delicate. However, it is easily verified that, with the particular choice

$$k_{w_2}(u_1) = k'_{w_2}|u_1|, \qquad k'_{w_2} > 0, \tag{66}$$

the control u_2 given by eqs. (62) and (63) coincides with the eigenvalue assignment control (59) associated with the linear time-invariant system (57). More precisely, there is a one-to-one correspondence between the parameters of the two control laws. One can thus apply classical linear control methods to determine these parameters in order to optimize the performance near the point $Z_2 = 0$, as will be illustrated in Sect. 4.1.4 in the application to the car-like robot.

According to Prop. 2, any sufficiently regular input $u_1(t)$ can be used for the regulation of Z_2 to zero, as long as it does not asymptotically tend to zero. This leaves the designer with some degrees of freedom in the choice of this input when addressing a path following problem. For instance, uniform exponential convergence of $\|Z_2\|$ to zero is obtained when $|u_1|$ remains larger than some positive number. Other sufficient conditions for exponential convergence of $\|Z_2\|$ to zero, which do not require u_1 to have always the same sign, may also be derived. For example, if $|\dot{u}_1|$ is bounded, then it is sufficient to have $|u_1|$ periodically larger than some positive number.

Finally, we note that the requirement that the signal $u_1(t)$ does not asymptotically tend to zero can be relaxed. In fact, non-convergence of $u_1(t)$ to zero under the assumption that $|\dot{u}_1|$ is bounded implies that $\int_0^t |u_1(\tau)|d\tau$ tends to infinity with t. When using the control (63) with the choice (66), divergence of this integral is the actual necessary condition for the asymptotic convergence of $\|Z_2\|$ to zero. This appears when the control (63) is interpreted as a stabilizing linear control for the time-invariant system (57) obtained by replacing the time variable by the aforementioned integral. However, this integral may still diverge when $u_1(t)$ tends to zero 'slowly enough' (like $t^{-\frac{1}{2}}$, for example). This indicates that $\|Z_2\|$ may converge to zero even when u_1 does, a fact that will be exploited next.

4.1.3 Point stabilization via smooth time-varying feedback

Proposition 2 suggests a simple way of determining a smooth time-varying feedback law which globally asymptotically stabilizes the origin $Z = 0$ of the whole system. In this case, the role of the control u_1 is to complement the action of the control w_2 (or, through eq. (62), u_2) in order to guarantee asymptotic convergence of z_1 to zero as well.

Proposition 3 *Consider the same control of Prop. 2*

$$w_2 = -k_{w_2}(u_1)z_n,$$

complemented with the following time-varying control

$$u_1 = -k_{u_1}z_1 + \eta(Z_2, t), \qquad k_{u_1} > 0, \tag{67}$$

where $\eta(Z_2, t)$ is a uniformly bounded and class C^{p+1} function ($p \geq 1$) with respect to time, with all successive partial derivatives also uniformly bounded with respect to time, and such that:

C1: $\eta(0,t) = 0$, *$\forall t$;*

C2: *There exist a time-diverging sequence $\{t_i\}$ $(i = 1, 2, \ldots)$ and a positive continuous function $\alpha(\cdot)$ such that*

$$\|Z_2\| \geq l > 0 \quad \Longrightarrow \quad \sum_{j=1}^{p} \left(\frac{\partial^j \eta}{\partial t^j}(Z_2, t_i)\right)^2 \geq \alpha(l) > 0, \quad \forall i.$$

Under the above controls, the origin $Z = 0$ is globally asymptotically stable.

Proof It has already been shown that the positive function $V(Z_2)$ used in Prop. 2 is nonincreasing along the closed-loop system solutions, implying that $\|Z_2\|$ is bounded uniformly with respect to initial conditions.

The first equation of the controlled system is

$$\dot{z}_1 = -k_{u_1} z_1 + \eta(Z_2, t). \tag{68}$$

This is the equation of a stable linear system subject to the bounded additive perturbation $\eta(Z_2, t)$. Therefore, existence and uniqueness of the solutions is ensured, and $|z_1|$ is bounded uniformly with respect to initial conditions.

From the expression of u_1, and using the regularity properties of $\eta(Z_2, t)$, it is found that u_1 is bounded along the solutions of the closed-loop system, together with its first derivative. Therefore, Prop. 2 applies; in particular, $V(Z_2)$ tends to some positive limit value V_{lim}, $\|\dot{Z}_2(t)\|$ tends to zero, and $Z_2(t)$ tends to zero if $u_1(t)$ does not.

We proceed now by contradiction. Assume that $u_1(t)$ does not tend to zero. Then, $\|Z_2(t)\|$ tends to zero. By uniform continuity, and in view of condition C1, $\eta(Z_2, t)$ also tends to zero. Equation (68) becomes then a stable linear system subject to an additive perturbation which asymptotically vanishes. As a consequence, $z_1(t)$ tends to zero implying, by the expression of u_1, that so does also $u_1(t)$, yielding a contradiction. Therefore, $u_1(t)$ must asymptotically tend to zero.

Differentiating the expression of u_1 with respect to time, and using the convergence of $u_1(t)$ and $\|\dot{Z}_2(t)\|$ to zero, we get

$$\dot{u}_1(t) = \frac{\partial \eta}{\partial t}(Z_2(t), t) + o(t), \qquad \text{with } \lim_{t \to +\infty} o(t) = 0.$$

Since $(\partial \eta / \partial t)(Z_2, t)$ is uniformly continuous (its time derivative is bounded), both $\dot{u}_1(t)$ and $(\partial \eta / \partial t)(Z_2, t)$ converge to zero (Barbalat's lemma). By using similar arguments, one can also show that the total time derivative of $(\partial \eta / \partial t)(Z_2(t), t)$ and

$(\partial^2\eta/\partial t^2)(Z_2(t),t)$ tend to zero. By repeating the same procedure as many times as necessary, one obtains that $(\partial^j\eta/\partial t^j)(Z_2,t)$ $(j=1,\ldots,p)$ tends to zero. Hence,

$$\lim_{t\to\infty}\sum_{j=1}^{p}\left(\frac{\partial^j\eta}{\partial t^j}(Z_2(t),t)\right)^2 = 0. \tag{69}$$

Assume now that $V_{\lim}$ is different from zero. This would imply that $\|Z_2(t)\|$ remains larger that some positive real number l (which can be calculated from $V_{\lim}$). Eq. (69) is then incompatible with the condition C2 imposed on the function $\eta(Z_2,t)$. Hence, $V_{\lim}$ is equal to zero and Z_2 asymptotically converges to zero. Then, by uniform continuity and using condition C1, $\eta(Z_2,t)$ also tends to zero. Finally, in view of the expression of u_1, asymptotic convergence of z_1 to zero follows immediately. ■

We point out that controls u_1 and u_2 resulting from Prop. 3 are smooth with respect to the state provided that the functions $\eta(Z_2,t)$ and $k_{w_2}(u_1)$ are themselves smooth. On the other hand, if $k_{w_2}(u_1)$ is chosen as in eq. (66), u_2 is only continuous.

In the overall controller, the choices related to u_2 (or w_2) can be made along the same lines indicated at the end of Sect. 4.1.2. In particular, the same control law (59) based on input scaling can be used. As for u_1, the gain k_{u_1} is typically chosen on the basis of an approximate linearization at the origin. Its second component $\eta(Z_2,t)$, which introduces an explicit time dependence, is referred to as the *heat function* in order to establish a parallel with probabilistic global minimization methods. The role of $\eta(Z_2,t)$ in the control strategy is fundamental, for it 'forces motion' until the system has not reached the desired configuration, thus preventing the state from converging to other equilibrium points.

The conditions imposed by Prop. 3 on the heat function η can be easily met. For example, the three following functions

$$\eta_1(Z_2,t) = \|Z_2\|^2\sin t \tag{70}$$

$$\eta_2(Z_2,t) = \sum_{j=0}^{n-2} a_j\sin(\beta_j t)\, z_{2+j} \tag{71}$$

$$\eta_3(Z_2,t) = \sum_{j=0}^{n-2} a_j\frac{\exp(b_j z_{2+j})-1}{\exp(b_j z_{2+j})+1}\sin(\beta_j t), \tag{72}$$

satisfy the conditions whenever $a_j\neq 0$, $b_j\neq 0$, $\beta_j\neq 0$, and $\beta_i\neq\beta_j$ for $i\neq j$. For the first function, this is obvious. For the second function, the proof can be found in [43]. The same proof basically applies to the third function, which has the additional feature of being uniformly bounded with respect to all its arguments. It should be noted that it is not strictly necessary to use time-periodic functions.

The choice of a suitable heat function is critical for the overall control performance. In general, it is observed that functions (71) and (72) behave better than (70) with respect to the induced asymptotic convergence rate. For the last two functions, the parameters a_j and b_j (which characterize the 'slope' of $\eta_2(Z_2,t)$ and $\eta_3(Z_2,t)$ near the origin $Z_2=0$) have much influence on the transient time needed for the solutions to converge to zero.

4.1.4 Application to the car-like robot

For the $(2,4)$ chained form (10) that pertains to the car-like robot, the non-trivial part of the change of coordinates (60) is defined by

$$z_4 = k_1\chi_2 + \chi_4,$$

since we have from eq. (55)

$$L_{h_1}z_3 = L_{h_1}\chi_3 = \chi_4.$$

The skew-symmetric form (61) becomes in this case

$$\begin{aligned}\dot z_1 &= u_1\\ \dot z_2 &= u_1 z_3\\ \dot z_3 &= -k_1u_1z_2 + u_1z_4\\ \dot z_4 &= -k_2u_1z_3 + w_2,\end{aligned}$$

with

$$w_2 = (k_1+k_2)u_1z_3 + u_2.$$

In view of Prop. 2 and eq. (66), the control input u_2 for the skew-symmetric form is chosen as

$$u_2 = -k'_{w_2}|u_1|z_4 - (k_1+k_2)u_1z_3 = -k_1k'_{w_2}|u_1|\chi_2 - (k_1+k_2)u_1\chi_3 - k'_{w_2}|u_1|\chi_4. \quad (73)$$

The value of the three gains k_1, k_2, and k'_{w_2} can be selected on the basis of the aforementioned correspondence between the structure of eq. (73) and the eigenvalue assignment control (59). In particular, by comparing the expression of u_2 with the input-scaled version (30) of the linear tracking controller, which assigns three coincident eigenvalues in $-\alpha|u_1|$ (with $\alpha>0$), we can solve for the three gains as

$$k_1 = \alpha^2/3, \qquad k_2 = 8\alpha^2/3, \qquad k'_{w_2} = 3\alpha.$$

In this association, one should remember that $\chi_2 = x_4$, $\chi_3 = x_3$, and $\chi_4 = x_2$. In particular, the following gain parameters have been used

$$k_1 = 1/3, \quad k_2 = 8/3, \quad k_{w_2} = 3,$$

corresponding to three eigenvalues in -1 for the input-scaled linear approximation.

As for the control input u_1, which is given by eq. (67), we have set $k_{u_1} = 10$, corresponding to an eigenvalue in -10 for the linear approximation of the x-error dynamics, and we have used the heat function η_2 with the following parameters

$$\begin{array}{lll} a_0 = 40, & a_1 = 20, & a_2 = 20, \\ \beta_0 = 1, & \beta_1 = 2, & \beta_2 = 3. \end{array}$$

The above controller has been simulated for a car-like robot with $\ell = 1$ m executing a parallel parking maneuver. The desired configuration is the origin of the state space, while the initial configuration at $t_0 = 0$ is

$$x(0) = 0, \quad y(0) = -5, \quad \theta(0) = 0, \quad \phi(0) = 0.$$

Figures 20–26 show respectively the cartesian motion of the vehicle, the time evolution of x, y, θ and ϕ, and the actual commands v_1 and v_2 applied to the car-like robot, obtained from u_1 and u_2 via the chained-form input transformation (9).

After performing several other numerical tests, we can conclude that:

- The motion is quite natural in the first phase of approaching.
- For any stabilization task, the final part of the motion resembles a parallel parking maneuver.
- Basically, the larger are the a_j parameters of the heat function η_2, the shorter is the transient time. On the other hand, more control effort is required far from the goal.
- The final convergence close to the goal is rather slow.

In order to achieve practical convergence to a small ball around the origin in finite time, a simpler, discontinuous heat function can be used. For example, we have chosen

$$\eta_4(z_2, z_3, z_4, t) = \begin{cases} k_\eta \sin t & \text{if } z_2^2 + z_3^2 + z_4^2 \geq \epsilon \\ 0 & \text{if } z_2^2 + z_3^2 + z_4^2 < \epsilon, \end{cases}$$

with $\epsilon = 10^{-3}$, $k_\eta = 20$, and modified one of the previous gains by setting $k_{u_1} = 5$. The obtained results are illustrated in Figs. 27–33. The norm of the final cartesian error is equal to $3.35 \cdot 10^{-2}$ m (only due to the y-coordinate), while the final values of θ and ϕ are $2.5 \cdot 10^{-3}$ rad and $5.5 \cdot 10^{-3}$ rad, respectively. This condition is reached in about 17 sec.

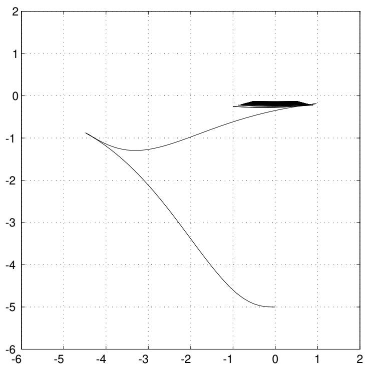

Figure 20: Point stabilization with time-varying feedback and heat function η_2: cartesian motion

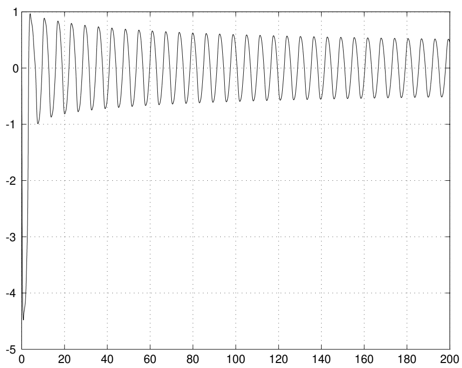

Figure 21: Point stabilization with time-varying feedback and heat function η_2: x (m) vs. time (sec)

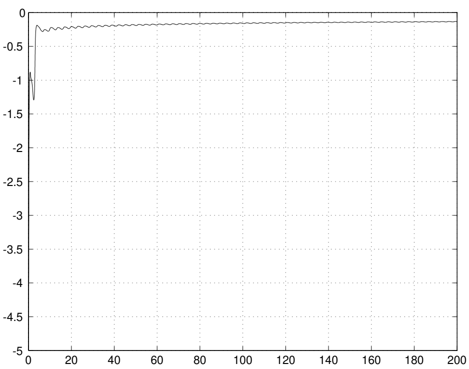

Figure 22: Point stabilization with time-varying feedback and heat function η_2: y (m) vs. time (sec)

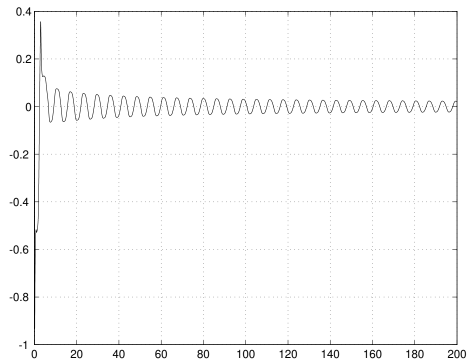

Figure 23: Point stabilization with time-varying feedback and heat function η_2: θ (rad) vs. time (sec)

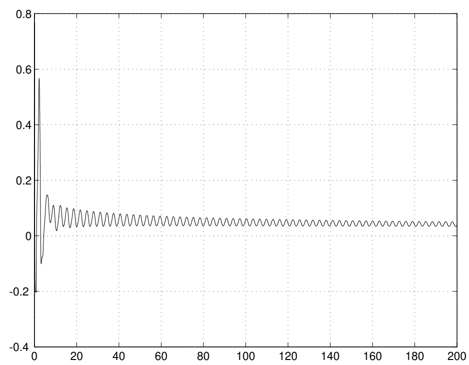

Figure 24: Point stabilization with time-varying feedback and heat function η_2: ϕ (rad) vs. time (sec)

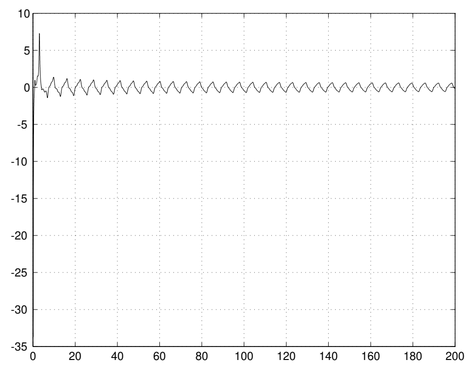

Figure 25: Point stabilization with time-varying feedback and heat function η_2: v_1 (m/sec) vs. time (sec)

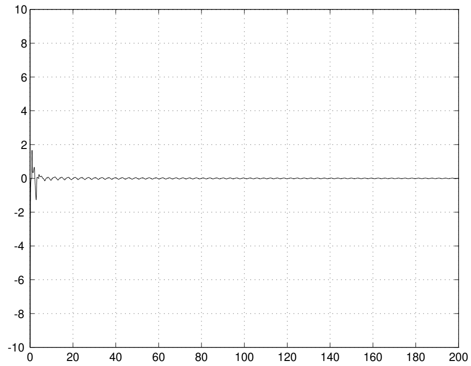

Figure 26: Point stabilization with time-varying feedback and heat function η_2: v_2 (rad/sec) vs. time (sec)

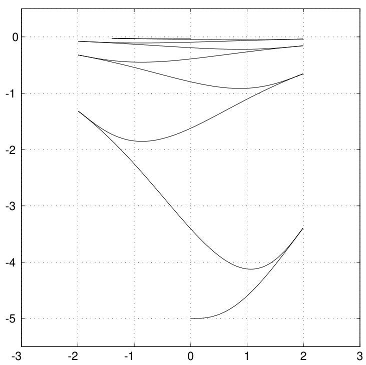

Figure 27: Point stabilization with time-varying feedback and heat function η_4: cartesian motion

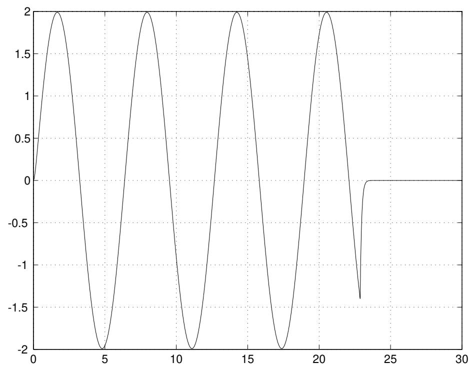

Figure 28: Point stabilization with time-varying feedback and heat function η_4: x (m) vs. time (sec)

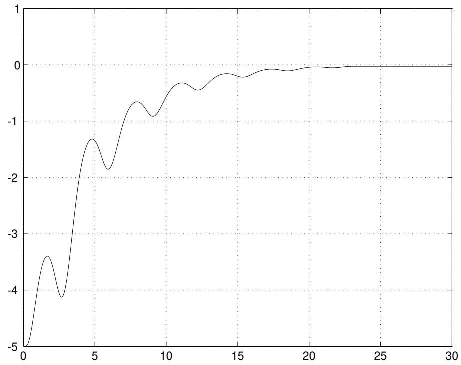

Figure 29: Point stabilization with time-varying feedback and heat function η_4: y (m) vs. time (sec)

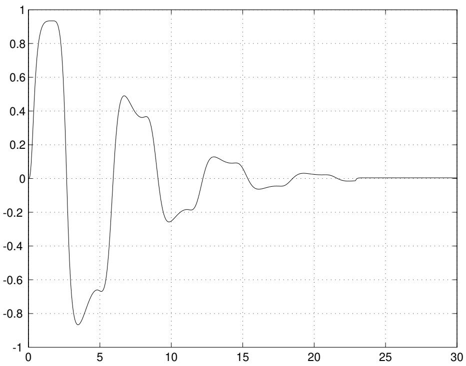

Figure 30: Point stabilization with time-varying feedback and heat function η_4: θ (rad) vs. time (sec)

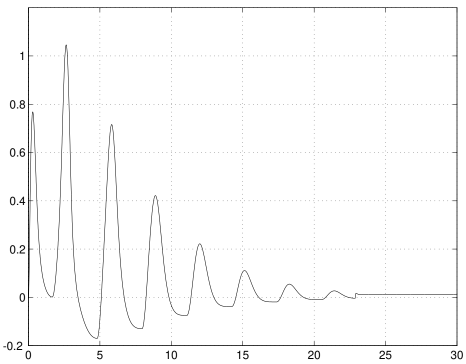

Figure 31: Point stabilization with time-varying feedback and heat function η_4: ϕ (rad) vs. time (sec)

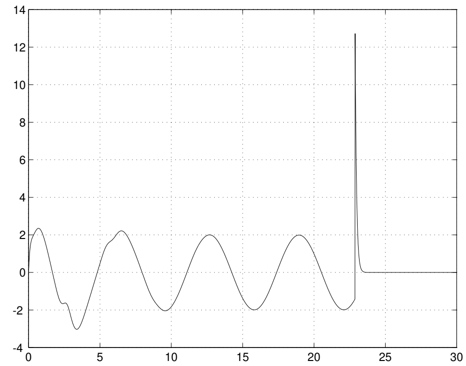

Figure 32: Point stabilization with time-varying feedback and heat function η_4: v_1 (m/sec) vs. time (sec)

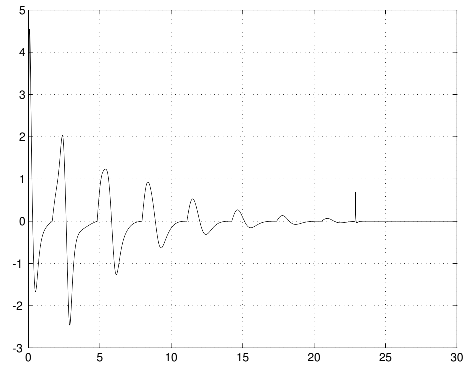

Figure 33: Point stabilization with time-varying feedback and heat function η_4: v_2 (rad/sec) vs. time (sec)

4.2 Control via nonsmooth time-varying feedback

We present next the design of a nonsmooth time-varying feedback controller that stabilizes the chained form to the origin. The contents of this section are based on [48] and [49]. The idea of decomposing the system into two parts and sequentially defining the two control inputs is very similar to the one pursued in Sect. 4.1. In fact, also this technique provides as a byproduct a solution to the path following problem. The fundamental difference here is that the feedback control law will depend, in addition to the exogenous time variable, on a piecewise-constant function of the state. Moreover, the actual construction of the control law for a subvector of dimension $n-1$ of the state is based on the so-called backstepping method.

4.2.1 Preliminaries

We begin with two definitions.

Definition 1 A function $h : I\!R^+ \mapsto I\!R^+$ is said to be of *class* $\mathcal{K}$ if it is strictly increasing and such that $h(0) = 0$. $\triangleleft$

Definition 2 For a nonlinear time-varying system

$$\dot{x} = f(x,t), \qquad x \in Q \subset I\!R^n, \quad t \geq t_0, \tag{74}$$

the equilibrium point x_e is globally $\mathcal{K}$-*exponentially stable* if there exists a positive constant λ (independent of t_0) and a function $h(\cdot)$ of class $\mathcal{K}$ such that all solutions $x(t)$ of eq. (74) satisfy

$$\|x(t) - x_e\| \leq h(\|x(t_0) - x_e\|)\, e^{-\lambda(t-t_0)}, \quad \forall x(t_0) \in Q,\ \forall t \geq t_0. \qquad \triangleleft$$

We note that a $\mathcal{K}$-exponentially stable system is uniformly asymptotically stable and, in addition, has an exponential rate of convergence. However, exponential stability in the sense of Lyapunov is stronger than the above property, because it involves a special function of class $\mathcal{K}$ which is linear, i.e.,

$$h(\|x(t_0) - x_e\|) = \bar{h}\|x(t_0) - x_e\|,$$

with $\bar{h} > 0$ independent from t_0 and $x(t_0)$. Nevertheless, the two properties are equivalent with respect to the rate of convergence, once the initial condition $x(t_0)$ is given.

The following technical lemma establishes sufficient conditions for obtaining exponential convergence in a time-varying system. Its proof can be found in [48].

Lemma 1 *Consider a scalar nonlinear time-varying system*

$$\dot{x} = -a(x,t)x + d(x,t), \qquad t \geq t_0, \tag{75}$$

under the following assumptions:

- *there exists a solution* $x(t)$ *of eq. (75) for any* $x(t_0)$ *and* $t \geq t_0$*;*
- $a(x,t)$ *is such that for all* $x(t)$

$$\left| \int_{t_0}^{t} (a(x(\tau),\tau) - \mu)\, d\tau \right| \leq P, \quad \forall t \geq t_0,$$

where μ *and* P *are some positive constants;*

– *$d(x,t)$ is bounded for all $x(t)$ as*

$$|d(x(\tau),\tau)| \le De^{-\gamma(t-t_0)}, \quad \forall t \ge t_0,$$

for some positive constants D and γ.

Then,

$$|x(t)| \le c\,(|x(t_0)| + D)e^{-(\beta-\varepsilon)(t-t_0)}, \quad \forall \varepsilon > 0,$$

where $\beta = \min\{\mu,\gamma\} > 0$ and $c = \max\{e^P, e^{2P}/\varepsilon\}$.

4.2.2 Backstepping control design

For convenience, we rewrite here the chained system (7)

$$\begin{aligned} \dot{x}_1 &= u_1 \\ \dot{x}_2 &= u_2 \\ \dot{x}_3 &= x_2 u_1 \\ &\vdots \\ \dot{x}_n &= x_{n-1} u_1, \end{aligned} \tag{76}$$

and partition its state as $X = (x_1, X_2)$, with $X_2 = (x_2, x_3, \ldots, x_n)$.

As previously noted, when u_1 is a predefined function of time, X_2 satisfies a linear time-varying equation driven by the input u_2. In the following, we will assume that a structure is assigned for the signal $u_1(t)$ and address the design of a feedback control law for u_2 so as to make $X_2 = 0$ a $\mathcal{K}$-exponentially stable equilibrium point. Later, we will add the variable x_1 to the picture and choose the specific form of control u_1 so as to obtain $\mathcal{K}$-exponential stability of $X = 0$ for the complete system.

The structure of u_1 is chosen by combining the simplicity of an open-loop command, which is updated as a function of the state only at discrete time instants, with the benefits of adding a time-varying exogenous signal. In particular, let a sequence of equidistant time instants $\{t_0, t_1, t_2, \ldots\}$ be defined as

$$t_h = hT, \qquad T = t_{h+1} - t_h > 0,$$

and define the control u_1 as

$$u_1(t) = k(X(t_h))f(t), \qquad \text{for } t \in [t_h, t_{h+1}). \tag{77}$$

This structure implies that the input is a function of the state X at time $t = t_h$, while during the interval (t_h, t_{h+1}) it is defined in an open-loop fashion. For the time being, no restrictions are put on the form of the function $k(\cdot)$ beside its boundedness. On the other hand, some assumptions are needed for function $f(t)$.

A1: $f(t) \in C^{\infty}$;

A2: $0 \leq f(t) \leq 1, \ \forall t \geq t_0$;

A3: $f(t_h) = 0, \ \forall t_h \in \{t_0, t_1, \ldots\}$;

A4: $\left| \int_{t_h}^{t} \left(f^{2(j-2)+1}(\tau) - \mu_j \right) d\tau \right| \leq P_j, \ \ \forall j \in \{3, \ldots, n\}, \ \forall t_h \in \{t_0, t_1, \ldots\}$,

where μ_j and P_j are positive constants.

Assumption A3 implies that $u_1(t_h) = 0$ for all $t_h \in \{t_0, t_1, \ldots\}$, and thus guarantees continuity of $u_1(t)$ with respect to time, even if function k is nonsmooth with respect to the state. Assumption A4 is more technical and is used to guarantee controllability of the linear time-varying subsystem and for proving exponential convergence of X_2 to zero by means of Lemma 1.

A simple periodic function satisfying the above assumptions is

$$f(t) = \frac{1 - \cos \omega t}{2}, \quad \omega = \frac{2\pi}{T}. \tag{78}$$

This function has a nonzero mean value, a fact which turns out to be important in order to have some 'control energy' sustaining the robot motion as long as an error is present, i.e., $X \neq 0$ (see the related remarks in Sect 4.1.3). However, $f(t)$ is not restricted to be periodic.

Using eq. (77), the lower part of system (76) becomes

$$\dot{X}_2 = \begin{bmatrix} \dot{x}_2 \\ \dot{x}_3 \\ \vdots \\ \dot{x}_{n-1} \\ \dot{x}_n \end{bmatrix} = \begin{bmatrix} u_2 \\ k(X(t_h)) f(t) x_2 \\ \vdots \\ k(X(t_h)) f(t) x_{n-2} \\ k(X(t_h)) f(t) x_{n-1} \end{bmatrix}, \quad t \in [t_h, t_{h+1}), \ h = 0, 1, \ldots. \tag{79}$$

In the following, we will often write $k = k(X(t_h))$ for compactness.

A feedback law for u_2 that renders $X_2 = 0$ exponentially convergent to zero (in fact, $\mathcal{K}$-exponentially stable) is now derived based on a *backstepping* method—a general technique for controlling systems in cascaded form [22]. Take the last equation in (79) and regard the variable x_{n-1} as a 'dummy' input to be used for driving exponentially the state x_n to its target $x_n^d = 0$. To this end, x_{n-1} should behave as a desired reference signal x_{n-1}^d which is chosen to satisfy

$$k f(t) x_{n-1}^d = -\lambda_n f^{2(n-2)+1}(t) x_n,$$

with arbitrary $\lambda_n > 0$, or equivalently

$$x_{n-1}^d = -\frac{\lambda_n}{k} f^{2(n-2)}(t) x_n. \tag{80}$$

This choice is convenient because, if $x_{n-1} = x_{n-1}^d$, the last equation in (79) becomes

$$\dot{x}_n = -\lambda_n f^{2(n-2)+1}(t) x_n.$$

By virtue of assumption A4, we may use Lemma 1 (with $a(t) = \lambda_n f^{2(n-2)+1}(t)$ and $d(t) = 0$) to infer that, at least with the nominal dummy input, x_n exponentially converges to zero. The convergence rate depends on the choice of the parameter λ_n.

During a transient phase, we will actually have a difference $\tilde{x}_{n-1} = x_{n-1} - x_{n-1}^d \neq 0$ leading to

$$\dot{x}_n = k f(t) x_{n-1}^d + k f(t) \tilde{x}_{n-1} = -\lambda_n f^{2(n-2)+1}(t) x_n + k f(t) \tilde{x}_{n-1}.$$

We can use again Lemma 1 (with $a(t) = \lambda_n f^{2(n-2)+1}(t)$ and $d(t) = k f(t) \tilde{x}_{n-1}$) to conclude that x_n exponentially converges to zero, provided that $|k f(t) \tilde{x}_{n-1}|$ is exponentially converging to zero as well. This will be guaranteed by the remaining steps of the recursive procedure.

Consider now the next to last equation in (79) and regard the variable x_{n-2} as the new dummy input, to be used for driving the state x_{n-1} to its target x_{n-1}^d specified by eq. (80). To obtain exponential convergence of $\tilde{x}_{n-1}$ to zero, x_{n-2} should behave as a desired reference x_{n-2}^d which is chosen to satisfy

$$k f(t) x_{n-2}^d = -\lambda_{n-1} f^{2(n-3)+1}(t)(x_{n-1} - x_{n-1}^d) + \dot{x}_{n-1}^d,$$

with arbitrary $\lambda_{n-1} > 0$. In fact, if $x_{n-2} = x_{n-2}^d$, the next to last equation in (79) gives

$$\dot{\tilde{x}}_{n-1} = -\lambda_{n-1} f^{2(n-3)+1}(t) \tilde{x}_{n-1},$$

and we can use again Lemma 1 to show that $\tilde{x}_{n-1}$ exponentially converges to zero, with rate depending on the parameter λ_{n-1}. This holds also when $\tilde{x}_{n-2} = x_{n-2} - x_{n-2}^d \neq 0$, provided that $|k f(t) \tilde{x}_{n-2}|$ is itself converging exponentially to zero.

Backstepping further, x_{n-3} will be regarded as the dummy input in the second to last equation in (79), and the same control design is repeated until we reach the top equation, in which the true input command u_2 is present. In this last step, the control input will be defined as

$$u_2 = -\lambda_2(x_2 - x_2^d) + \dot{x}_2^d. \tag{81}$$

With this choice, one can show (under additional assumptions on the function $k(\cdot)$ to be detailed later) that x_2 will converge exponentially to x_2^d, which in turn implies that x_3 converges exponentially to x_3^d, and so on until it is proven that x_n converges exponentially to $x_n^d = 0$.

At the end of this procedure, a reference value has been defined for each state component of X_2, namely

$$\begin{aligned} x_n^d &= 0 \\ x_{j-1}^d k(X(t_h)) f(t) &= -\lambda_j f^{2j-3}(t)(x_j - x_j^d) + \dot{x}_j^d, \quad \lambda_j > 0, \quad j = 3, \ldots, n. \end{aligned} \tag{82}$$

By expanding the time derivatives in eq. (82), the above reference values become a combination, weighted by powers of $f(t)$, of the state components in X_2. For example, in the case of the (2,4) chained form pertaining to a car-like robot we would obtain:

$$\begin{aligned} x_4^d &= 0 \\ x_3^d &= -\lambda_4 f^4(t) x_4 / k(X(t_h)) \\ x_2^d &= \left[-\lambda_3 f^3(t)(x_3 - x_3^d)/k(X(t_h)) + \dot{x}_3^d/k(X(t_h))\right]/f(t) \\ &= -\left[\left(\lambda_3 f^2(t) + \lambda_4 f^4(t)\right)/k(X(t_h))\right] x_3 - \left[\left(\lambda_3\lambda_4 f^6(t) + 4\lambda_4 f^2(t)\right)/k^2(X(t_h))\right] x_4. \end{aligned}$$

Note that the order of the exponent of function $f(t)$ in eq. (80) has been chosen large enough to guarantee that $f(t) = 0$ implies all $x_i^d = 0$. This choice forces the car-like robot to align its orientation and steering angle with the x-axis whenever it performs a cusp during the motion. In fact, the control u_1 may change sign only in correspondence to instants t in which $f(t) = 0$.

In order to obtain a compact expression for the control input u_2, the reference values (82) can be reorganized and written as

$$\begin{aligned} x_i^d &= f^{2(i-1)}(t) \sum_{j=i+1}^{n} \frac{g_{ij}}{k^{j-i}(X(t_h))} x_j, \qquad i = 2, \ldots, n-1, \\ x_n^d &= 0, \end{aligned} \tag{83}$$

where the functions $g_{ij} = g_{ij}(f, \dot{f}, \ldots, f^{(j-i-1)})$ are smooth with respect to their arguments and are defined recursively by

$$\begin{aligned} g_{n-1,n} &= -\lambda_n \\ g_{i-1,j} &= g_{ij}\left[\lambda_i f^{2(i-1)} + 2(i-1)\dot{f}\right] + f(\dot{g}_{ij} + g_{i,j+1} f) \\ g_{i-1,i} &= -\lambda_i + f^2 g_{i,i+1} \\ g_{ip} &= 0, \qquad\qquad \text{if } p \leq i \text{ or } p = n+1, \end{aligned} \tag{84}$$

for $i, j = 2, \ldots, n$, being

$$\dot{g}_{ij} = \sum_{m=0}^{j-i-1} \frac{\partial g_{ij}}{\partial f^{(m)}} f^{(m+1)}.$$

Summarizing eqs. (77), (81), (83), and (84), the following control structure is obtained

$$\begin{aligned} u_1 &= k(X(t_h))f(t) && (85)\\ u_2 &= \Gamma^T(k(X(t_h)),t)\,X_2, && (86) \end{aligned}$$

with

$$\Gamma^T(k,t) = [\Gamma_2(k,t)\ \ \ldots\ \ \Gamma_n(k,t)]$$

and

$$\begin{aligned} \Gamma_2(k,t) &= -\lambda_2 + f^3 g_{23}\\ \Gamma_j(k,t) &= f\left(\lambda_2 f g_{2j} + 2\dot{f} g_{2j} + f\dot{g}_{2j} + f^2 g_{2,j+1}\right)/k^{j-2}(X(t_h)), \quad j = 3,\ldots,n. \end{aligned}$$

4.2.3 Convergence results

The main convergence results for the above controller are now presented. We start by providing conditions on $k(\cdot)$ so as to guarantee exponential convergence to zero of the state X_2 in eq. (79), a result which provides a solution for the path following problem.

Proposition 4 *Consider system (79), where u_2 is given by eq. (86) and $f(t)$ has the properties A1–A4. Assume further that:*

- $k(0) = 0$;
- $X_2 \neq 0$ *implies* $k(X) \neq 0$;
- *there exists a constant K such that $|k(X)| \leq K$, $\forall X \in I\!R^n$;*
- *whenever $|k(X(t_h))| < K$, it is*

$$|k(X(t_h))| \geq \kappa_j |\tilde{x}_j(t)|^{\frac{1}{2(n-2)}}, \quad \forall j = 3,\ldots,n, \tag{87}$$

  where $\tilde{x}_j = x_j - x_j^d$ and κ_j is a positive constant.

Then, $X_2 = 0$ is $\mathcal{K}$-exponentially stable, i.e., there exist a constant $\lambda_{X_2} > 0$ and a function $h_{X_2}(\cdot,T)$ of class $\mathcal{K}$ such that

$$\|X_2(t)\| \leq h_{X_2}(\|X_2(t)\|,T)e^{-\lambda_{X_2}(t-t_0)}, \quad \forall X_2(t_0) \in I\!R^{n-1},\ \forall t \geq t_0.$$

Proof (sketch of) The first three assumptions are used to prove that the 'error' variables $\tilde{x}_2, \ldots, \tilde{x}_n$ converge to zero, i.e., each x_i $(i = 2, \ldots, n)$ converges to its reference value x_i^d defined by eq. (82). Lemma 1 is the main tool in this analysis, resulting in an exponential rate of convergence which can also be estimated. Then, one can show that the original states x_j $(j = 2, \ldots, n)$ can be expressed as a weighted sum of the error variables $\tilde{x}_r$ $(r = j+1, \ldots, n)$, essentially by reversing the construction of the x_i^d in eq. (83). Finally, by using eq. (87), $\mathcal{K}$-exponential stability of $X_2 = 0$ is obtained. ∎

A function $k(\cdot)$ satisfying the assumptions of the above proposition is given by

$$k(X) = \text{sat}\left(-\beta\left[x_1 + \text{sgn}(x_1)G\left(\|X_2\|\right)\right], K\right), \tag{88}$$

where

$$\text{sat}(z, K) = \begin{cases} z, & \text{if } |z| \leq K, \\ K\text{sgn}(z) & \text{if } |z| > K, \end{cases}$$

and

$$\begin{aligned} \text{sgn}(z) &= \begin{cases} 1, & \text{if } z \geq 0, \\ -1, & \text{if } z < 0, \end{cases} \\ G\left(\|X_2\|\right) &= \kappa \left\|X_2\right\|^{\frac{1}{2(n-2)}}, \\ \beta &= 1/\int_{t_h}^{t_{h+1}} f(\tau)d\tau, \end{aligned}$$

with κ a positive constant.

By using Prop. 4, one can finally establish global $\mathcal{K}$-exponential stability of the origin $X = 0$ of the total system in chained form (76), thus solving the point stabilization problem. We give this result without the proof, which is rather long and can be found in [49].

Proposition 5 *Consider system (76), where u_1 is given by eq. (85), with $k(X)$ chosen as in eq. (88) and $f(t)$ satisfying assumptions A1–A4, and u_2 is given by eq. (86). Then, $X = 0$ is $\mathcal{K}$-exponentially stable, i.e., there exist a constant $\lambda_X > 0$ and a function $h_X(\cdot, T)$ of class $\mathcal{K}$ such that*

$$\|X(t)\| \leq h_X(\|X(t_0)\|, T)e^{-\lambda_X(t-t_0)}, \quad \forall X(t_0) \in I\!R^n, \; \forall t \geq t_0.$$

Note the following facts.

- It can be shown that the class $\mathcal{K}$-function $h_X(\cdot, T)$ is not Lipschitz around the origin. In particular, its derivative tends to infinity when $\|X(t_0)\|$ approaches zero.

- The exponential convergence rate λ_X in Prop. 5 can be made arbitrarily fast by choosing β in eq. (88) and $\lambda_2, \ldots, \lambda_n$ in eq. (84) large enough. However, the time needed to drive x_1 to an arbitrarily small neighborhood of zero cannot be less than T. As a consequence, the class $\mathcal{K}$-function $h_X(\cdot, T)$ increases exponentially with the 'period' T. On the other hand, reducing T may result in a large control effort for some initial conditions.

- In the generic time interval $[t_h, t_{h+1})$, the control input u_1 is essentially open-loop being only a function of the state at time t_h, whereas the control input u_2 is a true feedback, for it depends continuously on the state variables X_2.

4.2.4 Application to the car-like robot

For the car-like robot in $(2,4)$ chained form, we present here explicit formulas for generating u_2 according to eq. (86). Let λ_2, λ_3, and λ_4 be three positive constants. Choose $f(t)$ as in eq. (78) and $k(X)$ as in eq. (88). We have

$$t_{h+1} - t_h = T = \frac{2\pi}{\omega} \qquad \text{and} \qquad \beta = \frac{1}{\int_{t_h}^{t_{h+1}} f(\tau) d\tau} = \frac{\omega}{\pi}, \quad \forall h.$$

Equations (84) give

$$\begin{aligned} g_{23} &= -\lambda_3 - \lambda_4 f^2 \\ \dot{g}_{23} &= -2\lambda_4 f \dot{f} \\ g_{24} &= -\lambda_4(\lambda_3 f^4 + 4\dot{f}) \\ \dot{g}_{24} &= -4\lambda_3\lambda_4 f^3 \dot{f} - 4\lambda_4 \ddot{f} \\ g_{25} &= 0, \end{aligned}$$

to be used in

$$\begin{aligned} \Gamma_2 &= -\lambda_2 + f^3 g_{23} \\ \Gamma_3 &= f\left[\lambda_2 f g_{23} + 2\dot{f} g_{23} + f\dot{g}_{23} + f^2 g_{24}\right] / k(X(t_h)) \\ \Gamma_4 &= f\left[\lambda_2 f g_{24} + 2\dot{f} g_{24} + f\dot{g}_{24} + f^2 g_{25}\right] / k^2(X(t_h)). \end{aligned}$$

The control input u_1 is provided by eq. (85).

The following parameters have been used in the various functions that define the control laws (85) and (86):

$$K = 2, \quad \omega = 1, \quad \kappa = 3, \quad \lambda_2 = \lambda_3 = \lambda_4 = 1.$$

Note that the first control input may switch only every 2π sec, i.e., at $t \in \{0, 2\pi, 4\pi, \ldots\}$.

The above controller has been simulated for a car-like robot with $\ell = 1$ m executing a parking maneuver. The desired configuration is the origin of the state space, while the initial configuration at $t_0 = 0$ is

$$x(0) = -1, \quad y(0) = -1, \quad \theta(0) = -\pi/4, \quad \phi(0) = 0. \tag{I}$$

Figures 34–40 show respectively the cartesian motion of the vehicle, the time evolution of x, y, θ and ϕ, and the actual commands v_1 and v_2 applied to the car-like robot, obtained from u_1 and u_2 through the chained-form input transformation (9). Similarly to the smooth time-varying controller of Sect. 4.1, the generated cartesian motion is natural and resembles a parallel parking maneuver in the final phase. Convergence to the desired configuration appears to be faster; however, $x = x_1$ converges much slower than the other variables y, θ and ϕ, which are related to $X_2 = (x_2, x_3, x_4)$. This behavior can be predicted by using Lemma 1.

These observations have been confirmed also by other simulations. For example, Figs. 41–47 show the results obtained by using the same controller in order to execute a reorientation maneuver. The desired configuration is again the origin of the state space, while the initial configuration is

$$x(0) = 0, \quad y(0) = 0, \quad \theta(0) = \pi/6, \quad \phi(0) = 0. \tag{II}$$

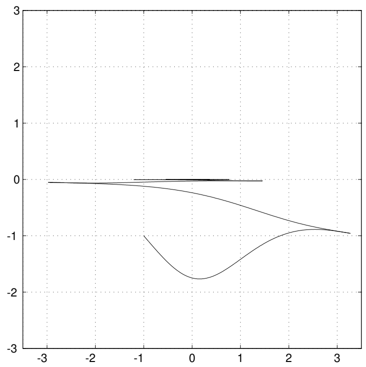

Figure 34: Point stabilization with nonsmooth time-varying feedback (I): cartesian motion

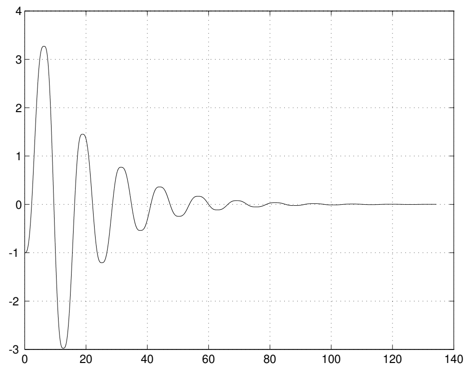

Figure 35: Point stabilization with nonsmooth time-varying feedback (I): x (m) vs. time (sec)

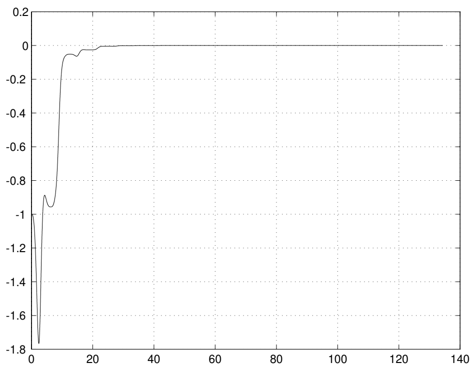

Figure 36: Point stabilization with nonsmooth time-varying feedback (I): y (m) vs. time (sec)

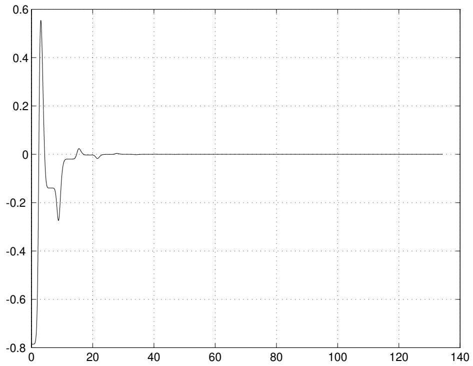

Figure 37: Point stabilization with nonsmooth time-varying feedback (I): θ (rad) vs. time (sec)

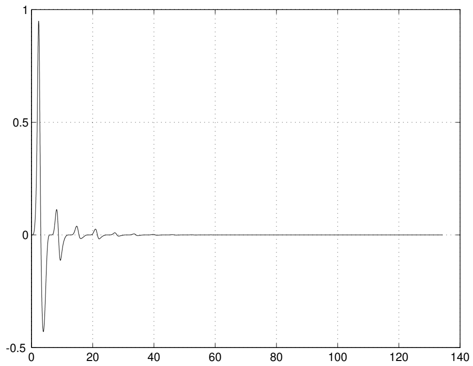

Figure 38: Point stabilization with nonsmooth time-varying feedback (I): ϕ (rad) vs. time (sec)

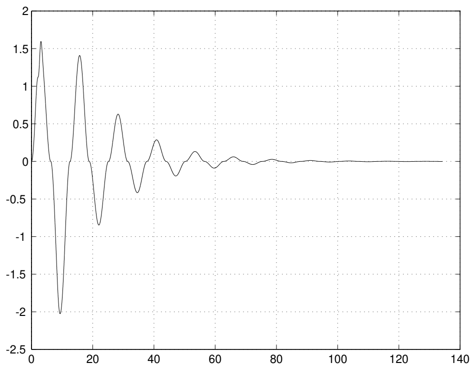

Figure 39: Point stabilization with nonsmooth time-varying feedback (I): v_1 (m/sec) vs. time (sec)

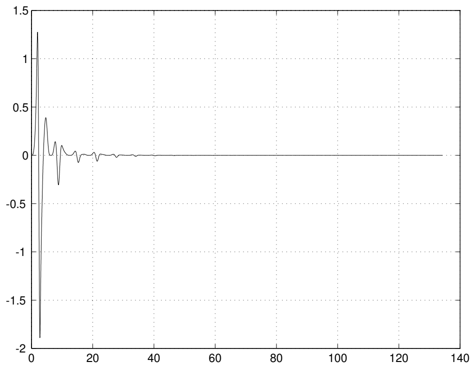

Figure 40: Point stabilization with nonsmooth time-varying feedback (I): v_2 (rad/sec) vs. time (sec)

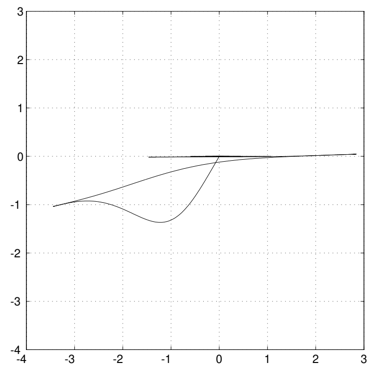

Figure 41: Point stabilization with nonsmooth time-varying feedback (II): cartesian motion

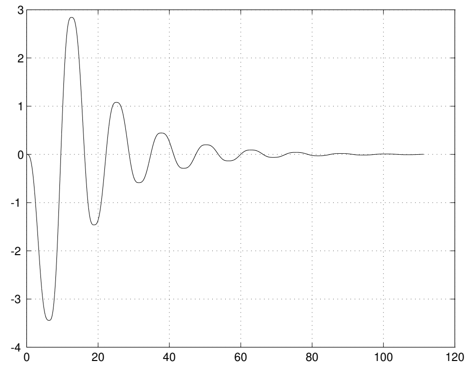

Figure 42: Point stabilization with nonsmooth time-varying feedback (II): x (m) vs. time (sec)

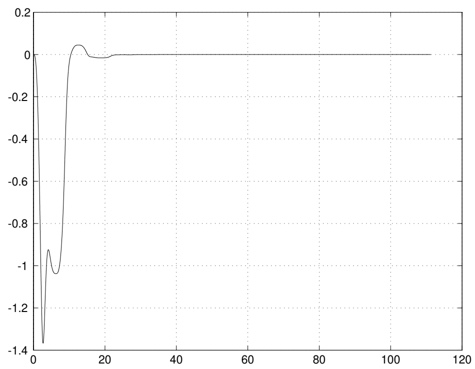

Figure 43: Point stabilization with nonsmooth time-varying feedback (II): y (m) vs. time (sec)

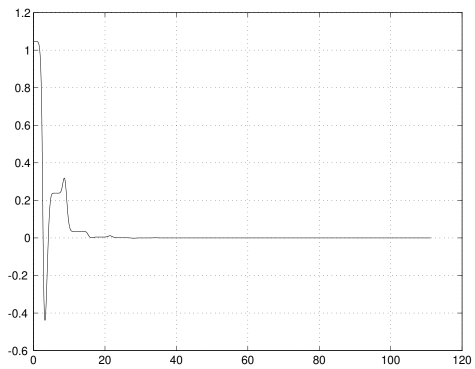

Figure 44: Point stabilization with nonsmooth time-varying feedback (II): θ (rad) vs. time (sec)

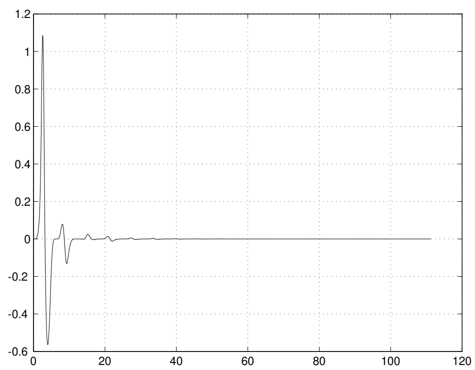

Figure 45: Point stabilization with nonsmooth time-varying feedback (II): ϕ (rad) vs. time (sec)

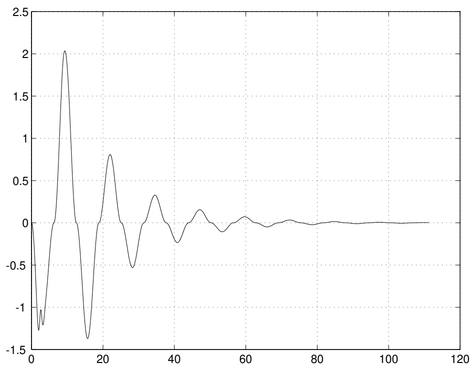

Figure 46: Point stabilization with nonsmooth time-varying feedback (II): v_1 (m/sec) vs. time (sec)

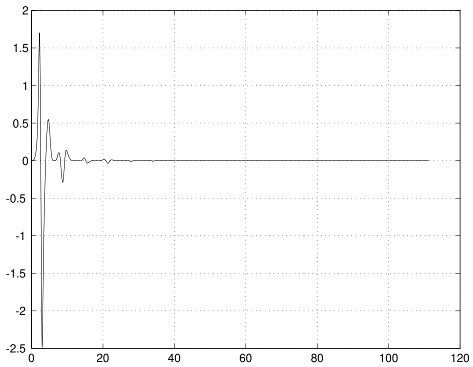

Figure 47: Point stabilization with nonsmooth time-varying feedback (II): v_2 (rad/sec) vs. time (sec)

4.3 About exponential convergence

The peculiar convergence behavior of both presented stabilizing methods deserves some comments. We have already pointed out in Sect. 2.2 that the failure of the linear controllability test for the car-like robot indicates that smooth exponential stability in the sense of Lyapunov cannot be obtained. Recall that (local) exponential stability means that the system trajectories $X(t)$ satisfy the following inequality

$$\|X(t)\| \leq K\|X(t_0)\|e^{-\lambda(t-t_0)}, \qquad \forall X(t_0) \in B, \quad \forall t \geq t_0, \tag{89}$$

with K, λ positive real numbers and B a neighborhood of the origin. The practical significance of this relationship is twofold: *(i)* small initial errors cannot produce arbitrarily large transient deviations since $\|X(t)\| \leq K\|X(t_0)\|$, and *(ii)* all solutions converge to zero exponentially.

While it is still unclear whether both properties can be simultaneously achieved for nonholonomic systems, one can still design a control law that guarantees at least one of the two. In the case of smooth time-varying feedback laws, such as the one presented in Sect. 4.1, it may be easily verified that

$$\|X(t)\| \leq K\|X(t_0)\|, \qquad \forall X(t_0), \quad \forall t \geq t_0, \tag{90}$$

holds for some positive constant K. However, when using the control law w_2 of Prop. 3, convergence to zero of $\|Z\|$ (and hence, of $\|X\|$) cannot be exponential. In fact, if this were the case, u_1 would itself converge to zero exponentially, and thus the integral $\int_0^t |u_1(\tau)|d\tau$ would not diverge. This is in contradiction with the fact that divergence of this integral is necessary for the asymptotic convergence of $\|Z_2\|$ to zero. As a matter of fact, it is only possible to show that

$$\|X(t)\| \leq K\|X(t_0)\|\rho(t), \qquad \text{with} \quad \rho(0) = 1, \ \lim_{t\to\infty} \rho(t) = 0, \tag{91}$$

where $\rho(t)$ is a decreasing function whose convergence rate is strictly less than exponential. This theoretical expectation is confirmed by the simulations results of Sect. 4.1.4. In particular, it has been observed [41] that smooth time-varying feedback control applied to a unicycle yields a convergence rate slower than $t^{-1/2}$ for most initial configurations, a fact that can be proven using center manifold theory.

On the other hand, existing nonsmooth feedback laws for nonholonomic systems do not guarantee uniform boundedness of the transient error ratio $\|X(t)\|/\|X(t_0)\|$. For example, the piecewise-continuous time-invariant feedback law proposed in [8] for the stabilization of a unicycle yields

$$\|X(t)\| \leq (K_1 + K_2\|X(t_0)\|)e^{-\lambda(t-t_0)}, \qquad \forall X(t_0), \quad \forall t \geq t_0, \tag{92}$$

with K_1, K_2 positive real numbers. All solutions converge to zero exponentially, but a small initial error or perturbation may produce transient deviations whose size is larger than some constant.

Similarly, we have seen that the nonsmooth time-varying feedback of Sect. 4.2 guarantees $\mathcal{K}$-exponential stability for general chained-form systems. Even if all solutions converge to zero exponentially, this type of asymptotic stability is weaker than property (89), in the sense that small initial errors or perturbations can produce transient deviations of much larger amplitude. Nevertheless, it is stronger than (92), for such deviations are not bounded below by some positive constant.

The above discussion may suggest that smooth time-varying feedback laws are somewhat less sensitive to initial errors than nonsmooth feedback laws. This degree of robustness is paid in terms of the asymptotic rate of convergence, which is not exponential. However, smooth time-varying feedback may be modified to achieve *practical* exponential stability, in the sense that the system state may be steered to any desired small neighborhood of the origin in arbitrary time. This fact is illustrated by the simulation results obtained with the heat function η_4 in Sect. 4.1.4.

5 Conclusions

We have presented and compared several feedback solutions for point stabilization, path following and trajectory tracking control tasks executed by a mobile robot with car-like kinematics.

The problem of accurate tracking of a persistent trajectory can be solved using either linear control synthesis, based on the approximate linearization of the system around the nominal trajectory, or nonlinear (static or dynamic) control synthesis, achieving exact linearization of the (input-output or full-state) closed-loop equations. Local exponential convergence to zero tracking error is obtained in the linear case, while global exponential convergence with prescribed error dynamics is guaranteed in the nonlinear case. In both approaches, the closed-loop controller consists of a nominal feedforward term and of an error feedback action.

For the stabilization to a fixed configuration, the use of new classes of time-varying nonlinear controllers has proven to be effective. From a theoretical point of view, time-varying feedback overcomes the obstruction on the existence of smooth time-invariant stabilizing control laws for nonholonomic systems. Two types of time-varying control laws were presented, respectively expressed by a smooth and a non-smooth function of the robot state. In both cases, we have recognized that path following can be formulated as a subproblem of point stabilization. The asymptotic rate of convergence of the smooth controller is lower than the exponential one obtained in the nonsmooth case. However, it may be questioned whether the theoretical convergence rate alone is a good measure of the overall control performance. In practice, what really matters is a rapid initial decay of the error to a small neighborhood of zero under realistic experimental conditions.

The reported numerical simulations have shown the benefit of feedback control in recovering from initial errors with respect to the desired fixed or moving target. In order to fully appreciate these results, we remark that errors (at the initial time or later) can be interpreted as the effect of an instantaneous disturbance acting on the system. Therefore, the robot motion under feedback control is robust with respect to such non-persistent disturbances.

Most of the results have been presented using a canonical transformation of the system into chained form. Although the use of chained forms is not needed in principle, it allows to obtain systematic results that can be extended beyond the considered case study of a car-like mobile robot. For example, the control results hold true also for a car towing N trailers, each attached at the midpoint of the rear axle of the previous one (zero hooking). On the other hand, the control problem for the general case of N trailers with nonzero hooking is still open, because a chained-form transformation is not available for this system.

Throughout this study, we have dealt with a first-order kinematic model of the mobile robot, in which velocities were assumed to be the control inputs. Extension to second-order kinematics, with accelerations as inputs, and inclusion of vehicle dynamics, with generalized forces as inputs, are possible. In particular, we point out that the nominal dynamics of the vehicle can be completely canceled by means of a nonlinear state feedback so as to obtain a second-order, purely kinematic problem.

Concerning the application of the proposed feedback controllers to real mobile robot systems, there are several non-ideal conditions that may affect the actual behavior of the controlled robot, notably: uncertain kinematic parameters of the vehicle (including, e.g., the wheels' radius); mechanical limitations such as backlash at the steering wheels and limited range of the steering angle; actuator saturation and dead-zone; noise and biases in the transformation from physical sensor data to the robot state; quantization errors in a digital implementation. Control robustness with respect to these kinds of uncertainties and/or disturbances is an open and challenging subject of research. For linear as well as nonlinear systems, Lyapunov exponential stability implies some degree of robustness with respect to perturbations. However, since this kind of stability has not been demonstrated for the point stabilization problem of nonholonomic systems, the connection between robustness properties and asymptotic (even exponential) rate of convergence is not yet well understood.

It should also be noted that perturbations acting on nonholonomic mobile robots are not of equal importance, depending on which component of the state is primarily affected. A deviation in a direction compatible with the vehicle mobility (e.g., sliding of the wheels on the ground) is clearly not as severe as a deviation which violates the kinematic constraints of the system (e.g., lateral skidding of the car-like robot). In any case, proprioceptive sensors may not reveal these perturbing actions and all the controllers presented in this chapter—which assume that the exact robot state is available—would fail in completing their task. A possible solution would be to close the feedback loop using exteroceptive sensor measurements, which provide absolute information about the robot location in its workspace. Currently, it is not clear whether the best solution would be to estimate the robot state from these measurements and then use the previous controllers, or to design new control laws aimed at zeroing the task error directly at the sensor-space level.

6 Further Reading

In addition to the references cited to support the results so far presented, many other related works have appeared in the literature. Hereafter, we mention some of the most significant ones.

A detailed reference on the kinematics of wheeled mobile robots is [2]. The dynamics of general nonholonomic systems was thoroughly analyzed in [31]. A controllability study for kinematic models of car-like robots with trailers was presented in [24], while stabilizability results for both kinematic and dynamic models of nonholonomic systems were given in [5, 7].

The problem of designing input commands that drive a nonholonomic mobile robot to a desired configuration has been first addressed through open-loop techniques. Purely differential-geometric approaches were followed in [23, 50], while the most effective solutions have been obtained by resorting to chained-form transformations and sinusoidal steering [28], or by using piecewise-constant functions as control inputs [26]. In [36] it was shown how the existence of differentially flat outputs can be exploited in order to design efficiently open-loop controls.

A number of works have dealt with the problem of controlling via feedback the motion of a unicycle. In fact, both discontinuous and time-varying feedback controllers were first proposed and analyzed for this specific kinematics. The trajectory tracking problem was solved in [39] by means of a local feedback action. Use of dynamic feedback linearization was proposed in [14]. A piecewise-continuous feedback with an exponential rate of convergence was presented in [8] for the point stabilization task, and later extended to the path following problem in [47]. Another piecewise-continuous controller, obtained through an appropriate switching sequence, was devised in [5]. The explicit inclusion of the exogenous time variable in a smooth feedback law was proposed in [38]. In [34], a hybrid stabilization strategy was introduced that makes use of a time-invariant feedback law far from the destination and of a time-varying law in its vicinity. The use of a discontinuous transformation in polar coordinates allowing to overcome the limitation of Brockett's theorem was independently proposed in [1] and [3] for the point stabilization problem; strictly speaking, these schemes are not proven to be stable in the sense of Lyapunov, for they only ensure exponential convergence of the error to zero. A survey of control techniques for the unicycle can be found in [9].

For car-like robots, the trajectory tracking problem was also addressed in [13] through the use of dynamic feedback linearization, and in [16] via flat outputs design and time-scaling. Path following via input scaling was proposed in [15, 37]. As for the point stabilization problem, the successful application of time-varying feedback to the case of car-like robots [43] has subsequently motivated basic research work aimed at exploring the potentialities of this approach. In particular, results have been obtained for the whole class of controllable driftless nonlinear systems in [11, 12], while general synthesis procedures were given in [33] for chained-form systems and in [35] for power-form systems; in the latter, the use of a nonsmooth but continuous time-varying feedback guarantees exponential convergence to the desired equilibrium point. Using an analysis based on homogeneous norms, similar results were obtained for driftless systems in [30], and for chained-form systems in [27] by means of a backstepping technique. Other related works include [17] and [51]. In the first, the problem of approximating a holonomic path via a nonholonomic one is solved by using time-periodic feedback control. In the second, the open-loop sinusoidal steering method is converted to a stabilization strategy, by adding to the nominal command a mixed discontinuous/time-varying feedback action.

Very few papers have explicitly addressed robustness issues in the control of nonholonomic systems. The robustness of a particular class of nonsmooth controllers based on invariant manifolds was analyzed in [10]. Robust stabilization of car-like robots in chained form was obtained in [4] and [25] by applying iteratively a contracting open-loop controller; exponential convergence to the desired equilibrium is obtained for small model perturbations. Another possible approach to the design of effective control laws in the presence of nonidealities and uncertainties is represented by learning control, as shown in [32].

Finally, the design of sensor-level controllers for nonholonomic mobile robots is at the beginning stage. The general concept of task-driven feedback control for holonomic manipulators is described in [40]. A first attempt to extend this idea to the point stabilization problem of a mobile robotic system can be found in [52].

References

[1] M. Aicardi, G. Casalino, A. Bicchi, and A. Balestrino, “Closed loop steering of unicycle-like vehicles via Lyapunov techniques,” *IEEE Robotics & Automation Mag.*, vol. 2, no. 1, pp. 27–35, 1995.

[2] J. C. Alexander and J. H. Maddocks, “On the kinematics of wheeled mobile robots,” *Int. J. of Robotics Research*, vol. 8, no. 5, pp. 15–27, 1989.

[3] A. Astolfi, “Exponential stabilization of a mobile robot,” *3rd European Control Conf.*, Roma, I, pp. 3092–3097, 1995.

[4] M. K. Bennani and P. Rouchon, “Robust stabilization of flat and chained systems,” *3rd European Control Conf.*, Roma, I, pp. 2642–2646, 1995.

[5] A. M. Bloch, M. Reyhanoglu, and N. H. McClamroch, "Control and stabilization of nonholonomic dynamic systems," *IEEE Trans. on Automatic Control*, vol. 37, no. 11, pp. 1746–1757, 1992.

[6] R. W. Brockett, "Asymptotic stability and feedback stabilization," in *Differential Geometric Control Theory*, R. W. Brockett, R. S. Millman, H. J. Sussmann (Eds.), Birkhäuser, Boston, MA, pp. 181–191, 1983.

[7] G. Campion, B. d'Andrea-Novel, and G. Bastin, "Modeling and state feedback control of nonholonomic mechanical systems," *30th IEEE Conf. on Decision and Control*, Brighton, UK, pp. 1184–1189, 1991.

[8] C. Canudas de Wit and O. J. Sørdalen, "Exponential stabilization of mobile robots with nonholonomic constraints," *IEEE Trans. on Automatic Control*, vol. 37, no. 11, pp. 1791–1797, 1992.

[9] C. Canudas de Wit, H. Khennouf, C. Samson, and O. J. Sørdalen, "Nonlinear control design for mobile robots," in *Recent Trends in Mobile Robots*, Y. F. Zheng (Ed.), World Scientific Publisher, 1993.

[10] C. Canudas de Wit and H. Khennouf, "Quasi-continuous stabilizing controllers for nonholonomic systems: Design and robustness considerations," *3rd European Control Conf.*, Roma, I, pp. 2630–2635, 1995.

[11] J.-M. Coron, "Global asymptotic stabilization for controllable systems without drift," *Mathematics of Control, Signals, and Systems*, vol. 5, pp. 295–312, 1992.

[12] J.-M. Coron, "Links between local controllability and local continuous stabilization," *2nd IFAC Symp. on Nonlinear Control System Design*, Bordeaux, F, pp. 477–482, 1992.

[13] B. d'Andrea-Novel, G. Bastin, and G. Campion, "Dynamic feedback linearization of nonholonomic wheeled mobile robots," *1992 IEEE Int. Conf. on Robotics and Automation*, Nice, F, pp. 2527–2532, 1992.

[14] A. De Luca and M. D. Di Benedetto, "Control of nonholonomic systems via dynamic compensation," *Kybernetica*, vol. 29, no. 6, pp. 593–608, 1993.

[15] E. D. Dickmanns and A. Zapp, "Autonomous high speed road vehicle guidance by computer vision," *10th IFAC World Congr.*, München, D, pp. 221–226, 1987.

[16] M. Fliess, J. Lévine, P. Martin, and P. Rouchon, "Design of trajectory stabilizing feedback for driftless flat systems," *3rd European Control Conf.*, Roma, I, pp. 1882–1887, 1995.

[17] L. Gurvits and Z. Li, "Smooth time-periodic feedback solutions for nonholonomic motion planning," in *Nonholonomic Motion Planning*, Z. Li, J. Canny (Eds.), Kluwer Academic Publishers, Norwell, MA, pp. 53–108, 1992.

[18] A. Isidori, *Nonlinear Control Systems*, 3rd Edition, Springer-Verlag, London, UK, 1995.

[19] T. Kailath, *Linear Systems*, Prentice-Hall, Englewood Cliffs, NJ, 1980.

[20] H. K. Khalil, *Nonlinear Systems*, Macmillan, New York, NY, 1992.

[21] I. V. Kolmanovsky, M. Reyhanoglu, and N. H. McClamroch, "Discontinuous feedback stabilization of nonholonomic systems in extended power form," *33rd IEEE Conf. on Decision and Control*, Lake Buena Vista, FL, pp. 3469–3474, 1994.

[22] M. Krstić, I. Kanellakopoulos, and P. Kokotović, *Nonlinear and Adaptive Control Design*, John Wiley & Sons, New York, NY, 1995.

[23] G. Lafferriere and H. J. Sussmann, "Motion planning for controllable systems without drift," *1991 IEEE Int. Conf. on Robotics and Automation*, Sacramento, CA, pp. 1148–1153, 1991.

[24] J.-P. Laumond, "Controllability of a multibody mobile robot," *IEEE Trans. on Robotics and Automation*, vol. 9, no. 6, pp. 755–763, 1993.

[25] P. Lucibello and G. Oriolo, "Stabilization via iterative state steering with application to chained-form systems," *35th IEEE Conf. on Decision and Control*, Kobe, J, pp. 2614–2619, 1996.

[26] S. Monaco and D. Normand-Cyrot, "An introduction to motion planning under multirate digital control," *31st IEEE Conf. on Decision and Control*, Tucson, AZ, pp. 1780–1785, 1992.

[27] P. Morin and C. Samson, "Time-varying exponential stabilization of chained systems based on a backstepping technique," *35th IEEE Conf. on Decision and Control*, Kobe, J, pp. 1449–1454, 1996.

[28] R. M. Murray and S. S. Sastry, "Nonholonomic motion planning: Steering using sinusoids," *IEEE Trans. on Automatic Control*, vol. 38, no. 5, pp. 700–716, 1993.

[29] R. M. Murray, "Control of nonholonomic systems using chained forms," *Fields Institute Communications*, vol. 1, pp. 219–245, 1993.

[30] R. M. Murray and R. T. M'Closkey, "Converting smooth, time-varying, asymptotic stabilizers for driftless systems to homogeneous, exponential stabilizers," *3rd European Control Conf.*, Roma, I, pp. 2620–2625, 1995.

[31] J. I. Neimark and F. A. Fufaev, *Dynamics of Nonholonomic Systems*, American Mathematical Society, Providence, RI, 1972.

[32] G. Oriolo, S. Panzieri, and G. Ulivi, "An iterative learning controller for nonholonomic robots," *1996 IEEE Int. Conf. on Robotics and Automation*, Minneapolis, MN, pp. 2676–2681, 1996.

[33] J.-B. Pomet, "Explicit design of time-varying stabilizing control laws for a class of controllable systems without drift," *Systems & Control Lett.*, vol. 18, pp. 147–158, 1992.

[34] J.-B. Pomet, B. Thuilot, G. Bastin, and G. Campion, "A hybrid strategy for the feedback stabilization of nonholonomic mobile robots," *1992 IEEE Int. Conf. on Robotics and Automation*, Nice, F, pp. 129–134, 1992.

[35] J.-B. Pomet and C. Samson, "Time-varying exponential stabilization of nonholonomic systems in power form," INRIA Rep. 2126, Dec. 1993.

[36] P. Rouchon, M. Fliess, J. Lévine, and P. Martin, "Flatness and motion planning: The car with n trailers," *2nd European Control Conf.*, Gröningen, NL, pp. 1518–1522, 1993.

[37] M. Sampei, T. Tamura, T. Itoh, and M. Nakamichi, "Path tracking control of trailer-like mobile robot," *1991 IEEE/RSJ Int. Work. on Intelligent Robots and Systems*, Osaka, J, pp. 193–198, 1991.

[38] C. Samson, "Velocity and torque feedback control of a nonholonomic cart," in *Advanced Robot Control*, C. Canudas de Wit (Ed.), Birkhäuser, Boston, MA, pp. 125–151, 1991.

[39] C. Samson and K. Ait-Abderrahim, "Feedback control of a nonholonomic wheeled cart in cartesian space," *1991 IEEE Int. Conf. on Robotics and Automation*, Sacramento, CA, pp. 1136-1141, 1991.

[40] C. Samson, M. Le Borgne, B. Espiau, *Robot Control: The Task Function Approach*," Oxford Science Publications, Oxford, UK, 1991.

[41] C. Samson and K. Ait-Abderrahim, "Feedback stabilization of a nonholonomic wheeled mobile robot, *1991 IEEE/RSJ Int. Work. on Intelligent Robots and Systems*," Osaka, J, pp. 1242-1247, 1991.

[42] C. Samson, “Path following and time-varying feedback stabilization of a wheeled mobile robot,” *2nd Int. Conf. on Automation, Robotics and Computer Vision*, Singapore, 1992.

[43] C. Samson, “Time-varying feedback stabilization of car-like wheeled mobile robots,” *Int. J. of Robotics Research*, vol. 12, no. 1, pp. 55–64, 1993.

[44] C. Samson, “Control of chained systems. Application to path following and time-varying point-stabilization of mobile robots,” *IEEE Trans. on Automatic Control*, vol. 40, no. 1, pp. 64–77, 1995.

[45] E. D. Sontag, “Feedback stabilization of nonlinear systems,” in *Robust Control of Linear Systems and Nonlinear Control*, M. A. Kaashoek, J. H. van Schuppen, A. C. M. Ran (Eds.), Birkhäuser, Cambridge, MA, pp. 61–81, 1990.

[46] O. J. Sørdalen, “Conversion of the kinematics of a car with n trailers into a chained form,” *1993 IEEE Int. Conf. on Robotics and Automation*, Atlanta, GA, vol. 1, pp. 382–387, 1993.

[47] O. J. Sørdalen and C. Canudas de Wit, “Exponential control law for a mobile robot: Extension to path following,” *IEEE Trans. on Robotics and Automation*, vol. 9, no. 6, pp. 837–842, 1993.

[48] O. J. Sørdalen, “Feedback control of nonholonomic mobile robots,” Ph. D. Thesis, The Norwegian Institute of Technology, Trondheim, NO, Mar. 1993.

[49] O. J. Sørdalen and O. Egeland, “Exponential stabilization of nonholonomic chained systems,” *IEEE Trans. on Automatic Control*, vol. 40, no. 1, pp. 35–49, 1995.

[50] H. J. Sussmann and W. Liu, “Limits of highly oscillatory controls and the approximation of general paths by admissible trajectories,” Tech. Rep. SYCON-91-02, Rutgers University, Feb. 1991.

[51] A. R. Teel, R. M. Murray, and G. Walsh, “Nonholonomic control systems: From steering to stabilization with sinusoids,” *31st IEEE Conf. on Decision and Control*, Tucson, AZ, pp. 1603–1609, 1992.

[52] D. Tsakiris, C. Samson, and P. Rives, “Vision-based time-varying stabilization of a mobile manipulator,” *6th Int. Conf. on Control, Automation, Robotics and Vision*, Singapore, 1996.